Supplementary Information

Sensitizer-enhanced two-photon patterning of biomolecules in photo-instructive hydrogels

Heike Krüger[1], Marvin Asido[2], Josef Wachtveitl[2], Robert Tampé[1], Ralph Wieneke[1,*]

[1]Institute of Biochemistry, Biocenter, Goethe University Frankfurt,
Max-von-Laue-Str. 9, 60438 Frankfurt a.M., Germany

[2]Institute of Physical and Theoretical Chemistry, Goethe University Frankfurt,
Max-von-Laue-Str. 7, 60438 Frankfurt a.M., Germany

[*]for correspondence: wieneke@em.uni-frankfurt.de

Table of Contents for Supplementary Information

Abbreviations

aa: amino acid, Boc: *tert*-butoxycarbonyl, CH: cyclohexane, COMU: (1-cyano-2-ethoxy-2-oxoethylidenaminooxy)-dimethylamino morpholinocarbenium hexafluoro-phosphate, DCM: dichlormethane, DIPEA: *N,N*-diisopropylethylamine DMEM: Dulbecco's modified eagle medium, DMF: *N,N*-dimethylformamide, DMSO: dimethylsulfoxide, EA: ethylacetate, EDT: 1,2-ethanedithiol, EDTA: ethylenediaminetetraacetic acid, Et_2O: diethyl ether, EtOH: ethanol, ex/em: excitation/emission, FCS: fetal calf serum, Fmoc: fluorenylmethoxycarbonyl, HEPES: 4-(2-hydroxyethyl)-1-piperazineethanesulfonic acid, His_6: *hexa*histidine, HOBt*H_2O: hydroxybenzotriazole monohydrate, HPLC: high performance liquid chromatography, MeCN: acetonitrile, MeOH: methanol, MQ water: Milli-Q water, MW: molecular weight, NHS: *N*-hydroxy succinimide, NMP: *N*-methyl-2-pyrrolidon, NTA: *N*-nitrilotriacetic acid, PBS: phosphate buffered saline, POI: protein/peptide of interest, ROI: region of interest, RP: reverse phase, RT: room temperature, s.d.: standard deviation, SE: standard error, SPPS: solid-phase peptide synthesis, t_R: retention time, ^{t}Bu: *tert*-butyl, TCEP: tris(2-carboxyethyl)-phosphine, TFA: trifluoroacetic acid, THF: tetrahydrofuran, TIPS: triisopropylsilane, *tris*NTA: *tris*-*N*-nitrilotriacetic acid.

1 Supplementary Methods

Materials. All reagents and solvents were of the best grade available, supplied by Fluka, Sigma Aldrich, Merck, Carl Roth, Cellendes, Acros Organics, ATTO-Tec, Santa Cruz or VWR, and were used without further purification. All Fmoc-amino acids were obtained from Iris Biotech and Fmoc-His(Trt) trityl chloride resin was obtained from Sigma Aldrich. HBS buffer consisted of 20 mM HEPES and 150 mM NaCl adjusted to pH 7.2 with NaOH. Unless otherwise stated, all reactions were performed under argon atmosphere using dry solvents (Sigma Aldrich). Analytical thin layer chromatography was performed on silica gel 60 plates with fluorescence indicator (254 nm, Merck). Column chromatography was performed on silica gel 60 (40-63 µm, Macherey-Nagel) using solvents of technical grade. COMU was obtained from Bachem. Carboxy-*tris*NTA(O^{t}Bu) was synthesized as previously described.[1] His_6-SGGGSGGG-C^{AF647}-A-NH_2 was synthesized by SPPS, and GFP-His_6 was kindly provided by Karl Gatterdam. ESI-MS spectra were recorded on VG Fisons with quadrupole analyzer. ^{1}H and ^{13}C-NMR spectra were recorded on a BRUKER AV250, AV400, AV500 or AV600. NMR-

Signals were calibrated on solvent signals: ^{1}H-NMR: $CDCl_3$: 7.26 ppm; DMSO-d_6: 2.50 ppm; ^{13}C-NMR: $CDCl_3$: 77.16 ppm; DMSO-d_6: 39.52 ppm. ^{1}H-NMR data are presented as chemical shift in ppm (multiplicity, coupling constant, integration). The following abbreviations are used in reporting NMR-Data: s, singlet; d, doublet; t, triplet; q, quartet; dd, doublet of doublets; m, multiplet.

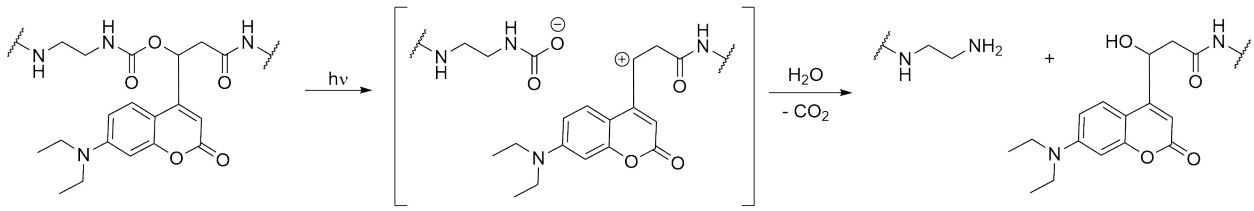

Supplementary Figure 1. Cleavage mechanism of DEAC-based photolabil protecting group inside TPA-*tris*NTA (adapted from Klán *et al.*).[2] After absorption of light, the DEAC enters the excited state where a tight ion pair (TIP) between the carbamate anion and the carbocation of the coumarin-methyl group is formed. Subsequently, the TIP gets separated by addition of water from the solvent, whereby a primary amine is released *via* decarboxylation under formation of the DEAC alcohol.

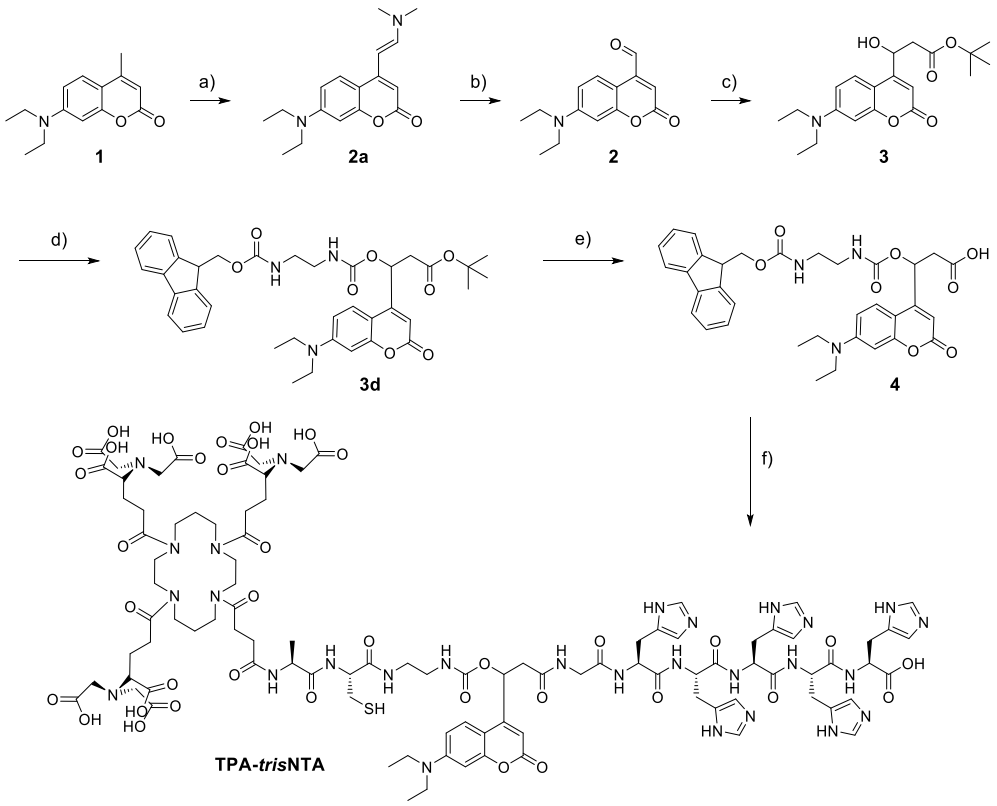

Supplementary Figure 2. Synthesis of TPA-*tris*NTA.

1.1 Chemical synthesis

(*E*)-7-(Diethylamino)-4-[2-(dimethylamino)vinyl]-2*H*-chromen-2-one (2a). DMF-DMA (862 µL, 0.77 g, 6.49 mmol) was added to commercially available 7-diethylamino-4-methyl-2-oxo-2H-chromen (1 g, 4.32 mmol) in 3 mL anhydrous DMF. The solution was stirred at 160 °C for 24 h, cooled down to RT, and poured in ice-cold MQ water (10 mL). The suspension was filtrated, and the filter cake was washed three times with ice-cold MQ water (10 mL). The filter cake was lyophilized to dryness to obtain the product as a yellow solid (98% yield, 1.22 g, 4.26 mmol). ^{1}H NMR (400 MHz, $CDCl_3$) δ[ppm] = 7.63 (d, *J* = 8.2 Hz, 1H), 7.29 (s, 1H), 6.83 – 6.49 (m, 2H), 5.95 (s, 1H), 5.22 (d, *J* = 12.9 Hz, 1H), 3.42 (q, *J* = 7.0 Hz, 4H), 3.02 (s, 6H), 1.22 (t, *J* = 7.1 Hz, 6H). ESI-MS MW calcd for $C_{17}H_{23}N_2O_2$ $[M+H]^+$ 287.18 Da, found 287.18 Da.

7-(Diethylamino)-2-oxo-2*H*-chromene-4-carbaldehyde (2). Sodium periodate (2.69 g, 12.5 mmol) was added to a stirred suspension of **2a** (1.20 g, 4.19 mmol) in water:THF (1:1, v/v, 90 mL). After 24 h stirring at RT, the suspension was filtered over silica gel and washed with EA until the silica gel remained colorless. The organic solvents were evaporated under reduced pressure. The residue was washed with DCM (3x 50 mL) and the combined organic layers were dried over Na_2SO_4, filtrated and evaporated under reduced pressure. The crude product was purified by column chromatography (CH/EA 3:1, v/v). **2** was obtained as a dark red solid (85% yield, 0.87 g, 3.55 mmol). ^{1}H NMR (400 MHz, $CDCl_3$) δ[ppm] = 10.03 (s, 1H), 8.32 (d, *J* = 9.2 Hz, 1H), 6.67 (dd, *J* = 9.2, 2.4 Hz, 1H), 6.57 (d, *J* = 2.4 Hz, 1H), 6.47 (s, 1H), 3.43 (q, *J* = 7.1 Hz, 4H), 1.22 (t, *J* = 7.1 Hz, 6H). ^{13}C-NMR (126 MHz, $CDCl_3$) δ[ppm] = 192.41, 161.52, 157.17, 149.59, 143.83, 127.47, 119.00, 111.29, 100.25, 46.30, 12.26. ESI-MS MW calcd for $C_{14}H_{16}NO_3$ $[M+H]^+$ 246.11 Da, found 246.13 Da.

***tert*-Butyl 3-(7-(diethylamino)-2-oxo-2H-chromen-4-yl)-3-hydroxypropanoate (3).** *tert*-Butyl bromoactetate (221 µL, 1.5 mmol) was added to a suspension of activated zinc powder (0.131 g, 2.0 mmol) in 3 mL dry DMF at 0 °C. The reaction mixture was stirred at 0 °C for 1 h followed by addition of **2** (0.245 g, 1.0 mmol). After 1 h, the reaction was stopped by adding 10 mL saturated NH_4Cl solution. The mixture was filtered through silica gel to remove remaining zinc. The filtrate was extracted three times with 10 mL Et_2O. The combined organic layers were dried over Na_2SO_4 and after filtration the solvent was removed under reduced pressure. The crude product was purified by column chromatography (DCM/acetone 20:1, v/v). The product was obtained as a yellow solid (75% yield, 270 mg,

0.75 mmol). ^{1}H NMR (250 MHz, $CDCl_3$) δ[ppm] = 7.38 (d, *J* = 9.0 Hz, 1H), 6.58 (dd, *J* = 9.0, 2.6 Hz, 1H), 6.52 (d, *J* = 2.6 Hz, 1H), 6.30 (s, 1H), 5.34 (d, *J* = 9.6 Hz, 1H), 3.56 (d, J = 3.5 Hz, 1H), 3.41 (q, J = 7.1 Hz, 4H), 2.76 (dd, J = 16.8, 2.9 Hz, 1H), 2.60 (dd, J = 16.8, 9.4 Hz, 1H), 1.49 (s, 9H), 1.20 (t, *J* = 7.1 Hz, 6H). ^{13}C-NMR (101 MHz, $CDCl_3$) δ[ppm] = 171.40, 162.22, 156.53, 155.64, 150.30, 124.72, 108.69, 105.88, 100.00, 98.18, 82.33, 66.21, 44.81, 42.24, 28.12, 12.43. ESI-MS MW calcd for $C_{20}H_{28}NO_5$ $[M+H]^+$ 362.19 Da, found 362.18 Da.

***tert*-Butyl 10-(7-(diethylamino)-2-oxo-2H-chromen-4-yl)-1-(9H-fluoren-9-yl)-3,8-dioxo-2,9-dioxa-4,7-diazadodecan-12-oate (3d).** DIPEA (225 µL, 1.32 mmol) was added dropwise to a solution of **3** (119 mg, 0.33 mmol) and triphosgene (118 mg, 0.39 mmol) in 1.5 mL of anhydrous THF at 0 °C. The reaction mixture was stirred at RT for 90 min. The solvent was evaporated to obtain the chloroformate **3** as a pale-yellow solid, which was used without additional purifications. Quantitative conversion was assumed and used for calculations of further reactions.

Mono-Fmoc ethylenediamine hydrochloride (210 mg, 0.66 mmol) and DIPEA (225 µL, 1.32 mmol) were added to a solution of the chloroformate **3** (139 mg, 0.33 mmol) in 2 mL anhydrous 1.4-dioxane. The reaction mixture was stirred for 1 d at RT and the solvent was evaporated. The residue was dissolved in 4 mL water/EA (1:1, v/v) and the organic layer was washed with water (2 mL) and brine (2 mL). The organic layer was dried over Na_2SO_4. After filtration, the solvent was removed under reduced pressure. The crude product was purified by column chromatography (CH/EA 1:1, v/v). The product was obtained as a pale yellow solid (56% yield, 127 mg, 0.19 mmol). ^{1}H-NMR (600 MHz, DMSO-d_6) δ[ppm] =7.88 (d, *J* = 7.4 Hz, 2H), 7.67 (d, *J* = 7.5 Hz, 2H), 7.52 (s, 1H), 7.47 (d, *J* = 9.1 Hz, 1H), 7.40 (t, *J* = 7.3 Hz, 2H), 7.31 (t, *J* = 7.3 Hz, 2H), 7.28 (s, 1H), 6.74 (d, *J* = 9.1 Hz, 1H), 6.55 (s, 1H), 6.11 (dd, *J* = 9.0, 3.5 Hz, 1H), 5.96 (s, 1H), 4.33 – 4.24 (m, 2H), 4.19 (t, *J* = 6.9 Hz, 1H), 3.42 (q, *J* = 7.0 Hz, 4H), 3.09-3.01 (m, 4H), 2.86-2.83 (m, 1H), 2.69 – 2.58 (m, 1H), 1.38 (s, 9H), 1.11 (t, *J* = 7.0 Hz, 6H). ^{13}C-NMR (101 MHz, DMSO-d_6) δ[ppm] =168.58, 161.07, 156.48, 156.39, 155.16, 154.68, 150.75, 144.24, 144.18, 141.05, 141.04, 129.25, 127.91, 127.37, 125.47, 125.45, 125.39, 121.70, 120.42, 109.39, 105.10, 104.62, 99.86, 97.42, 90.81, 81.10, 76.67, 70.13, 67.76, 65.68, 65.66, 47.04, 44.33, 27.93, 12.62. ESI-MS MW calcd for $C_{38}H_{44}N_3O_8$ $[M+H]^+$ 670.31 Da, found 670.19 Da.

10-(7-(Diethylamino)-2-oxo-2H-chromen-4-yl)-1-(9H-fluoren-9-yl)-3,8-dioxo-2,9-dioxa-4,7-diazadodecan-12-oic acid (4). 3d (500 mg, 0.75 mmol) was solved in ice-cold DCM:TFA (1:1, v/v, 8 mL) and stirring was continued for 1 h. The reaction mixture was concentrated under reduced pressure and the crude product was purified by column chromatography using RP-C_{18} silica (water: MeCN, 1:1, 1% TFA v/v%). The product was obtained as a pale yellow solid (73% yield, 337 mg, 0.55 mmol). ^{1}H-NMR (500 MHz, DMSO-d_6) δ[ppm] = 7.88 (d, *J* = 7.5 Hz, 2H), 7.67 (d, *J* = 7.4 Hz, 2H), 7.54 (s, 1H), 7.47 (d, *J* = 9.1 Hz, 1H), 7.40 (t, *J* = 7.4 Hz, 2H), 7.33-7.30 (m, 3H), 6.73 (dd, *J* = 9.1, 2.4 Hz, 1H), 6.54 (d, *J* = 2.3 Hz, 1H), 6.11 (dd, *J* = 9.3, 3.1 Hz, 1H), 5.95 (s, 1H), 4.34 – 4.25 (m, 2H), 4.20 (t, *J* = 6.8 Hz, 1H), 3.42 (q, *J* = 6.9 Hz, 4H), 3.09-3.02 (m, 4H), 2.85 (dd, *J* = 16.4, 3.3 Hz, 1H), 2.72 – 2.62 (m, 1H), 1.11 (t, *J* = 7.0 Hz, 6H). ^{13}C-NMR (126 MHz, DMSO-d_6) δ[ppm] = 171.23, 161.24, 156.61, 156.54, 155.34, 155.31, 150.88, 144.40, 144.34, 141.19, 128.06, 127.53, 125.63, 125.50, 120.57, 109.54, 105.24, 104.43, 97.56, 68.00, 65.83, 47.17, 44.47, 12.78. ESI-MS MW calcd for $C_{34}H_{36}N_3O_8$ $[M+H]^+$ 614.25 Da, found 614.25 Da.

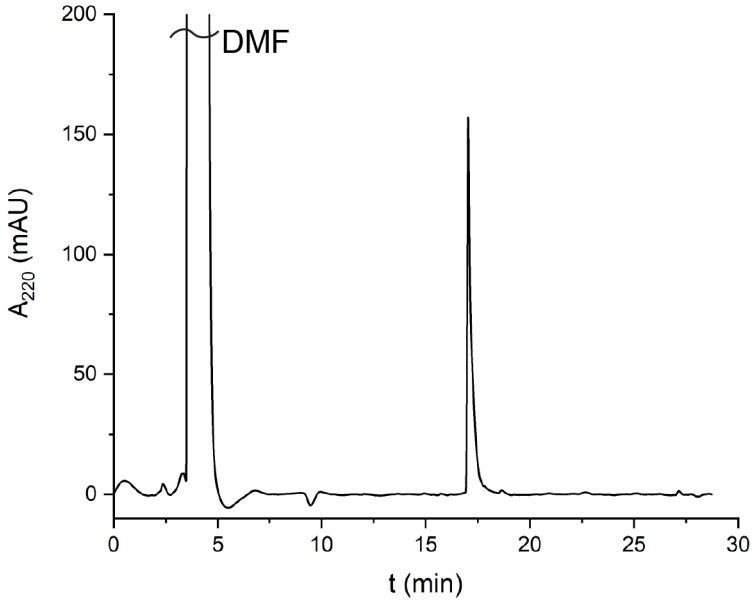

Supplematary Figure 3. RP-C_{18}-HPL chromatogram of purified 4. t_R= 17.0 min[meth.1]

1.2 Solid phase peptide synthesis of TPA-*tris*NTA

TPA-*tris*NTA was synthesized on a preloaded Fmoc-His(Trt)-Wang resin (Sigma Aldrich, Germany) as a solid support with a *Liberty Blue* microwave peptide synthesizer (CEM, Germany) using the method described in **Supplementary Table 1**. All coupling reactions except coupling of **4** (single coupling) were done twice with 0.2 M of Fmoc-protected aa, 0.5 M DIC, and 0.5 M HOBt monohydrate in DMF. Deprotection was performed with 20% (v/v%) Piperidine in DMF. O^{t}Bu-protected carboxy-*tris*NTA was coupled manually to the growing peptide chain. Therefore, 3 eq. **4** were preactivated for 5 min with 3 eq. COMU and 6 eq. DIPEA in DMF (0.3 M) and then added to the resin for 1 h at RT under shaking. Cleavage of **TPA-*tris*NTA** from the resin was achieved using 95% TFA and 5% of scavengers (water, EDT; 2.5% v/v of each) as cleavage cocktail for 2 h, precipitated in ice-cold Et_2O, pelleted, and washed with ice-cold Et_2O. This was repeated five times. Finally, the pellet was dissolved in ^{t}BuOH/H_2O (4:1, v/v), lyophilized and purified with RP-C_{18}-HPLC (method 2) with a Perfectsil C_{18} column (250×10 mm, 300 ODS, 5 µm, MZ-Analytical, Mainz, Germany) at a constant flow rate of 4 mL/min to obtain **TPA-*tris*NTA** as a yellow solid (yield 10%). HR ESI-MS MW calcd for $C_{98}H_{133}N_{28}O_{37}S$ $[M+H]^+$ 2325.9102 Da, found $[M+H]^+$ 2325.9130 Da, $[M+2H]^{2+}$ 1163.4692 Da, $[M+3H]^{3+}$ 775.9784 Da, $[M+4H]^{4+}$ 582.2252 Da.

Supplementary Table 1. SPPS method for synthesis of **TPA-*tris*NTA**

aa	microwave power (W)	time (s)	temperature (°C)
Fmoc-His(Trt)-COOH	34	390	50
Fmoc-Gly-COOH	30	330	60
4	10	2520	30
Fmoc-Cys(Trt)-COOH	30	330	60
Fmoc-Ala-COOH	30	330	60

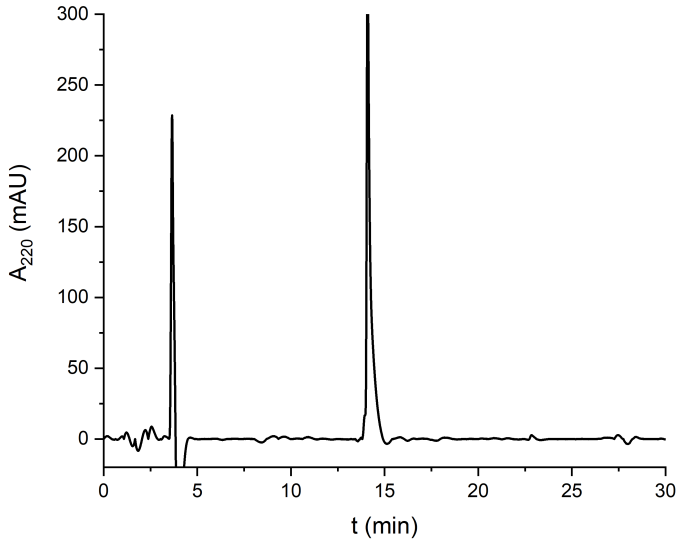

Supplematary Figure 4. RP-C_{18}-HPL chromatogram of purified TPA-*tris*NTA. t_R= 14.0 min[method 2]

1.3 Reverse phase -C_{18}-high performance liquid chromatography

RP-C_{18}-HPL chromatograms were recorded on a *Jasco HPLC 2000* equipped with a MD-2018 and AS-2057. The mobile phase consisted of buffer A: 0.1% TFA (aq.) and buffer B: MeCN + 0.1% TFA. Purification was performed by semi-preparative RP-C_{18}-HPLC (PerfectSil C_{18} column 250 x 10 mm 300 ODS, 5 µm, MZ Analytical, Germany) with 4 mL/min. Analytical RP-C_{18}-HPLC was conducted on PerfectSil C_{18} column 250 x 4 mm 300 ODS, 5 μm, (MZ Analytical, Germany) with 1 mL/min.

Supplementary Table 2. RP-C_{18}-HPLC gradients. **4** was analyzed using method 1 and **TPA-*tris*NTA** was analyzed and purified with method 2.

method 1		
t (min)	0.1% TFA (aq.) (%)	MeCN + 0.1% TFA (%)
0	95	5
20	0	100
25	0	100
26	95	5
30	95	5

method 2		
t (min)	0.1% TFA (aq.) (%)	MeCN + 0.1% TFA (%)
0	95	5
30	30	70
31	0	100
35	0	100
36	95	5
40	95	5

1.4 UV-Vis absorption and fluorescence emission spectra

Absorption spectra were recorded at 25 °C on an *Agilent Cary 100* UV/Vis instrument with 1 nm interval from 250 to 800 nm. Emission spectra were obtained from 400 to 800 nm with excitation at 380 nm at a *Varian Cary Eclipse* fluorescence spectrometer. Freshly prepared samples of **2**, **3**, **4** and **TPA-*tris*NTA** (50-100 µM) in HBS buffer:MeCN (1:1, v/v) were used to perform all UV–Vis absorption and fluorescence measurements. For each compound, multiple absorption and fluorescence spectra were measured. Normalized spectra are shown in Figure 1a and Supplematary Figure 5. The path length of the cuvette was 1 cm and the baseline correction was carried out by subtraction of the background signal of HBS buffer:MeCN (1:1, v/v).

1.5 Fluorescence quantum yield of TPA-*tris*NTA

The fluorescence quantum yield ϕ_F was determined by using an integrative sphere (ILF-835, Jasco, Germany) attached to a fluorescence spectrometer (FP-8500, Jasco, Germany). Spectra were taken in the range from 250 nm to 900 nm with a spectral resolution of 2 nm. The PMT voltage was adjusted to 440 V to achieve the maximum fluorescence signal without saturation of the detector. For reference and sample measurements, 4x10 mm Quartz cuvettes were employed. To avoid reabsorption effects, the OD of TPA-*tris*NTA in HBS buffer was adjusted to ~0.1 (10 mm optical path length). HBS buffer was used as reference. The reference signal (mainly the stray light of the buffer and the cuvette) was subtracted from the sample signal. By calculating the ratio between the residual fluorescence and the excitation integrals (Supplematary Figure 7), a ϕ_F of 15% was determined. Processing and

quantum yield calculation were performed with the Jasco software package (*Spectra Manager Suite*).

1.6 Reversibility of POI trapping

After two-photon photo-patterning at 800 nm, the gel was washed with HBS buffer (20 mM HEPES/NaOH, 150 mM NaCl pH 7.2, 25 °C), incubated with 10 mM $NiCl_2$ (1 mL in HBS buffer) followed by tethering of GFP-His_6 (300 nM). To remove unbound protein, the gel was gently agitated in HBS buffer. POI release was induced by incubating the gel with 1 mL of 500 mM imidazole in HBS buffer at RT. For POI reattachment, the gel was washed five times with HBS buffer and immersed to 300 nM fluorescently labeled POI His_6-AF647, followed by washing with HBS buffer (Supplematary Figure 9). Visualization of POI binding, release and reattachment was monitored by confocal laser scanning microscopy.

1.7 Long-term stability and persistence of photo-patterns

To study the long-term stability of POI tethering, 3D arbitrary protein patterns (bird) were generated by two-photon excitation and visualized by tethering of 300 nM fluorescently labeled His_6-AF647. Prior to imaging, the gel was washed with HBS buffer. Images of the photo-structured gel were immediately taken after POI immobilization (day 0) and 10 days later by confocal laser scanning microscopy. For analysis, the fluorescence intensity emanating from the His_6-POI-AF647 was determined with *Fiji*[3] at four distinct spots within the respective ROIs. Comparison of the mean fluorescence intensities at day 0 and day 10 revealed that POI pattern is still persistent after prolonged time intervals and that 19% ± 1% of starting POI fluorescence signal remained (Supplematary Figure 10). Imaging conditions (laser power, detector amplification and pinhole) were kept constant and applied to both hydrogels.

1.8 Z-axis profile analysis

Via confocal laser scanning microscopy, z stacks (35 slices, z step width 1 µm) of the photo-structured ROIs were recorded. The z stacks covered the entire photo-activated area and the fluorescence intensity within the voxel was measured. Orthogonal cross sections (x/z plane) of the two-photon patterned ROIs were created with *Fiji*[3], followed by generating a line scan profile along the z axis of the two-photon patterned hydrogels. Representative intensity

profiles of hydrogels activated in presence of 100 µM ATTO390 or 50 µM rhodamine B were shown in Supplematary Figure 15.

1.9 Full width at half maximum (FWHM) determination

After recording a z stack of a photo-structured ROI and generating an orthogonal cross section (x/z plane) of the two-photon activated area, a line scan profile along the z coordinate was created. The FWHM in z direction was determined by fitting a Gaussian to the line scan profile (Supplementary Table 3). All analyses were performed with *OriginLab* and software.[3]

Supplementary Table 3. Calculated FWHM values for hydrogels activated in presence of HBS buffer, 100 µM ATTO390 or 50 µM rhodamine B.

	Hydrogel 1 **HBS buffer** **12 s illumination**	**Hydrogel 2** **100 µM ATTO390** **12 s illumination**	**Hydrogel 3** **50 µM rhodamine B** **12 s illumination**
Laser power (mW)	**FWHM ± SE (µm)**	**FWHM ± SE (µm)**	**FWHM ± SE (µm)**
1.5	4.9 ± 0.7	5.7 ± 0.2	6.8 ± 0.1
3.1	6.3 ± 0.2	6.1 ± 0.2	9.4 ± 0.1
5.5	7.6 ± 0.1	n.d.	n.d.

n.d.: not determined

1.10 Cell culture

HeLa Kyoto cells were maintained in DMEM with 4.5 g/L glucose (Gibco), supplied with 10% (v/v) FCS. HeLa Flp-In™ T-Rex™ cells stably expressing the hormone neuropeptide Y2 receptor modified with a *C*-terminal mEGFP and a *N*-terminal His_6-tag (His_6-Y_2R^{mEGFP}; kindly provided by Dr. M. Florencia Sánchez) were cultured in DMEM containing 4.5 g/L glucose (Gibco), supplied with 10% (v/v) tetracycline free FCS (Gibco), 1 µg/mL blasticidine S (ThermoFisher), 50 µg/mL hygromycin B (Sigma Aldrich) and 436 µg/mL GlutaMAX (Gibco). To induce receptor expression, cell medium was replaced by fresh medium containing 0.1 µg/mL tetracycline (Fluka) 16 h before embedding in hydrogels. For passaging, cells were washed with PBS (Gibco) and detached from the culture dish with 0.05% trypsin/0.02% EDTA/PBS (GE Healthcare). Cell lines were stored in a humidified tissue culture incubator at 37 °C and 5% CO_2. Mycoplasma contamination tests were carried out regularly, following the guidelines described.[4]

1.11 Cell viability assessed in cell-laden hydrogels (Apoptosis analysis)

Supplementary Table 4. Hydrogel composition for cell apoptosis analysis

component	concentration (mM)	volume (µL)
10x CB buffer pH 7.2		3.0
Mal-PVA SG	30.0	2.5
TPA-*tris*NTA	20.0	0.8
dithiol linker	20.0	3.0
water		11.3
cells		10.0
total volume		30.6

1.12 Cytotoxicity effect of photo-sensitizers

24 h before assaying cytotoxicity of the photo-sensitizers, 200 µL of a HeLa cell suspension ($5x10^6$ cells/mL) in DMEM supplemented with 4.5 g/L glucose and without Phenol Red (Gibco), supplied with 10% (v/v) FCS, were seeded per well into two 96-well cell culture microplates (Greiner Bio-One, Austria). The plates were incubated at 37 °C in a fully humidified atmosphere of 5% CO_2. The next day, the medium was carefully aspirated and 100 µL of a of photoenhancer solution with increasing concentration (ATTO390: 50, 100, 500 µM; rhodamine B: 50, 100 µM) and dissolved in HBS buffer was added. One 96-well plate was kept under ambient light whereas the second plate was illuminated for 1 min at 365 nm by 185 mW/cm^2 with a custom made 96-well LED setup. Subsequently, both plates were incubated at 37 °C and 5% CO_2. After 2 h, the cells were carefully aspirated and fresh culture medium was added. 24 h later, the culture medium was removed and 50 µL serum-free media and 50 µL 3-(4,5-dimethylthiazol-2yl)-2,5-dipehnyltetrazolium bromide (MTT) solution (5 mg/mL in DPBS, sterile filtrated; Abcam) were added to each well. The plates were incubated for 3 h under standard cell culture conditions. After incubation, 150 µL MTT Solvent (Abcam) was added. MTT formazan was dissolved by thoroughly pipetting up and down. Absorbance was measured at 590 nm with 20 readings per well using a *ClarioStar* microplate reader (BMG Labtech). Background absorbance (from wells treated as above but without cells) was subtracted and the untreated control cells were assumed as 100%. Cell viability was calculated as: relative cell viability = [(experimental value – background

value)/(untreated control value-background value)] x100%. All conditions were tested as triplicates per sample/control (Supplementary Figure 17).

2 Supplementary Figures

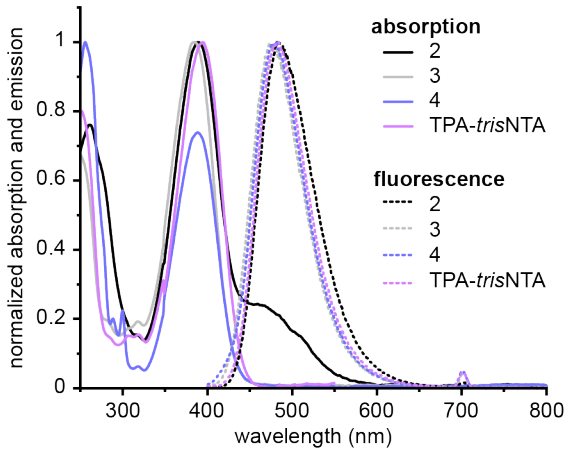

Supplematary Figure 5. Normalized absorption and emission spectra of TPA-*tris*NTA and compounds 2-4. Absorption spectra of TPA-*tris*NTA and compound 2-4 in HBS buffer/MeCN (1:1) were recorded from 250-800 nm with a 1 nm interval. Emission spectra of TPA-*tris*NTA and compound 2-4 were obtained from 400-800 m (λ_{ex}= 380 nm). The unaltered absorbance and emission spectra demonstrate that the light-absorbing properties of DEAC incorporated into TPA-*tris*NTA are not affected. Only DEAC derivative 2 showed a second maximum at 460 nm due to its aldehyde substitution in 3-position.

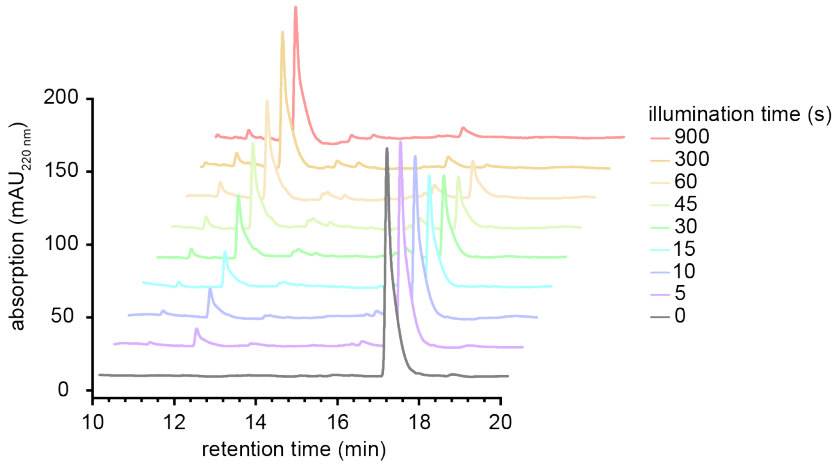

Supplematary Figure 6. Photolysis analysis of the DEAC ß-amino acid entity 4 in solution. Time-dependent photo-activation of 4 was monitored by RP-C_{18}-HPLC analysis at 220 nm [method 2] after illuminating the sample for 0-900 s at 405 nm. Disappearance of the starting material and formation of uncaged amino acid was observed. Caged DEAC and uncaged DEAC elute at 17.0 min and 12.0 min, respectively.

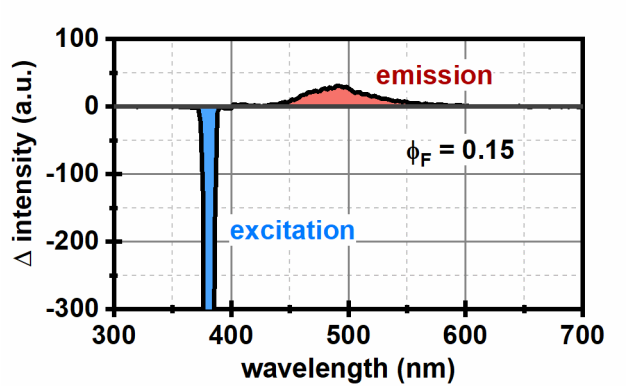

Supplematary Figure 7. Fluorescence quantum yield determination of TPA-*tris*NTA. The ϕ_F of 0.15 was calculated by determining the ratio between the emission integral and the excitation integral. Difference intensities of the reference-corrected sample spectrum were obtained by fluorescence measurement with an integrating sphere. For better visualization the excitation peak (blue) is not shown completely.

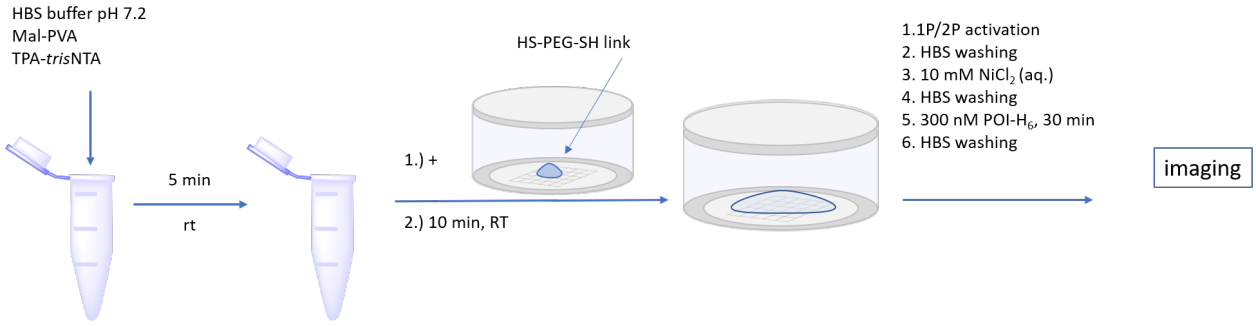

Supplematary Figure 8. Workflow for photo-patterning of TPA-*tris*NTA functionalized hydrogels with His_6-tagged POIs. TPA-*tris*NTA was conjugated to Maleimide-PVA in HBS buffer pH 7.2 and incubated for 5 min. This solution was added to the dithiol linker, positioned in the middle of a gridded *ibidi* slide. Hydrogel network formation was allowed to proceed for 10 min. Photo-patterning was performed by one-/ or two-photon excitation followed by washing with HBS buffer, *tris*NTA loading *via* incubation with 10 mM $NiCl_2$ and washing with HBS buffer. POI tethering in photo-patterned areas was realized by addition of 300 nM POI-His_6 to the gel for 30 min. Visualization of POI organization was conducted on a confocal laser scanning microscope.

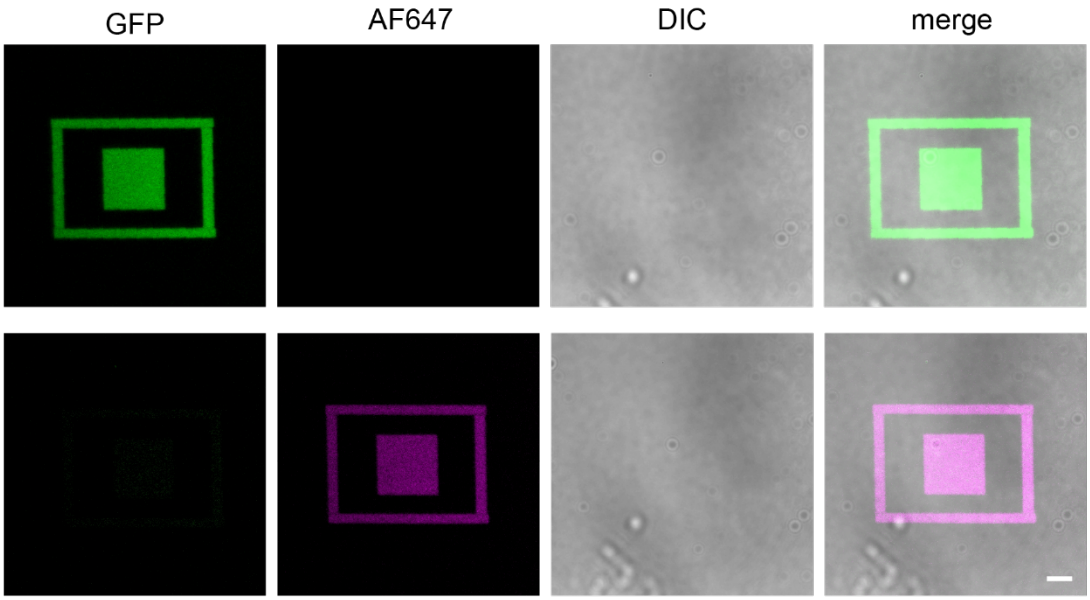

Supplematary Figure 9. Reversibility of POI-binding in photo-instructive TPA-*tris*NTA hydrogels. Two-photon structuring was performed by laser-assisted lithography followed by GFP-His_6 immobilization and visualization via confocal laser scanning microscopy. Before imidazole treatment, POI binding to the photo-structured ROIs was observed (green channel, upper row). After incubation with 500 mM imidazole, no fluorescence signal for GFP-His_6 was detected (green channel, lower row), demonstrating the displacement of the His-tagged POI by the competitor imidazole. Via incubation with 300 nM His_6-AF647, POI photo-pattern reassembly was realized, indicated by the fluorescence signal emanating from His_6-AF647 (magenta channel; lower row). This verifies the reversibility and regeneration of the photo-patterns in TPA-*tris*NTA functionalized hydrogels, facilitated by the non-covalent *tris*NTA/His_6-tag interaction. Images were taken by confocal laser scanning microscopy. DIC stands for Differential Interference Contrast. Scale bar: 10 µm.

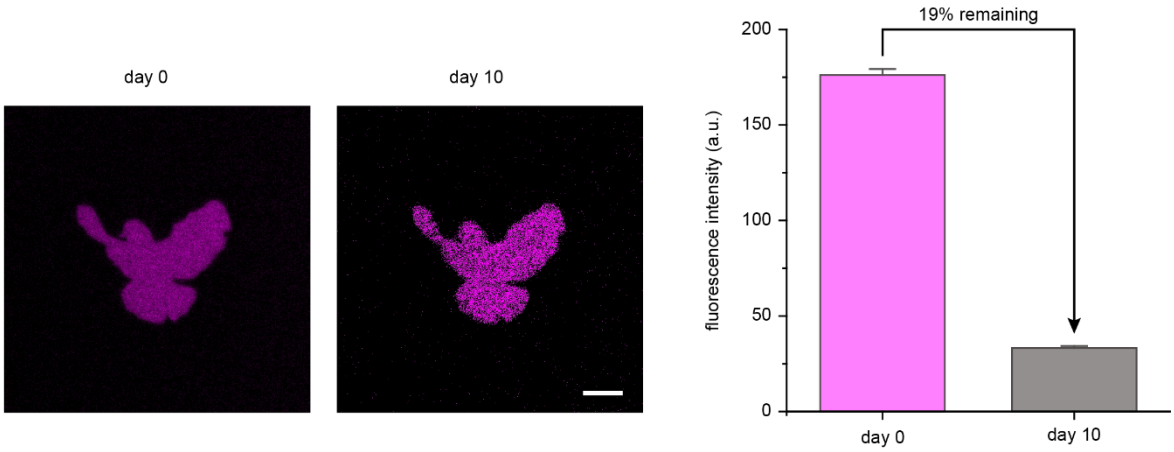

Supplematary Figure 10. Long-term stability and persistence of POI organization in photo-instructive TPA-*tris*NTA hydrogels. 3D arbitrary protein patterns (bird) were generated by laser-assisted two-photon structuring followed by POI tethering of 300 nM His_6-AF647. A strong fluorescence intensity emanating from His_6-AF647 within the bird shaped ROI was detected at day 0. After prolonged time periods (day 10), a diminished fluorescence signal intensity was measured. Bar diagram of the analysis of the fluorescence intensity at day 0 and day 10 showed a 5-fold decreased fluorescence signal after 10 days. Due to the high-affinity interaction between *tris*NTA and the His_6-tagged POI, 19% of the POI assembly remains tethered to the photo-structured ROI after extended time periods. Imaging was performed by confocal laser scanning microscopy in HBS buffer (20 mM HEPES/NaOH, 150 mM NaCl, pH 7.2, 25 °C). On day 10, the buffer was exchanged against fresh HBS buffer before imaging. Scale bar: 10 µm.

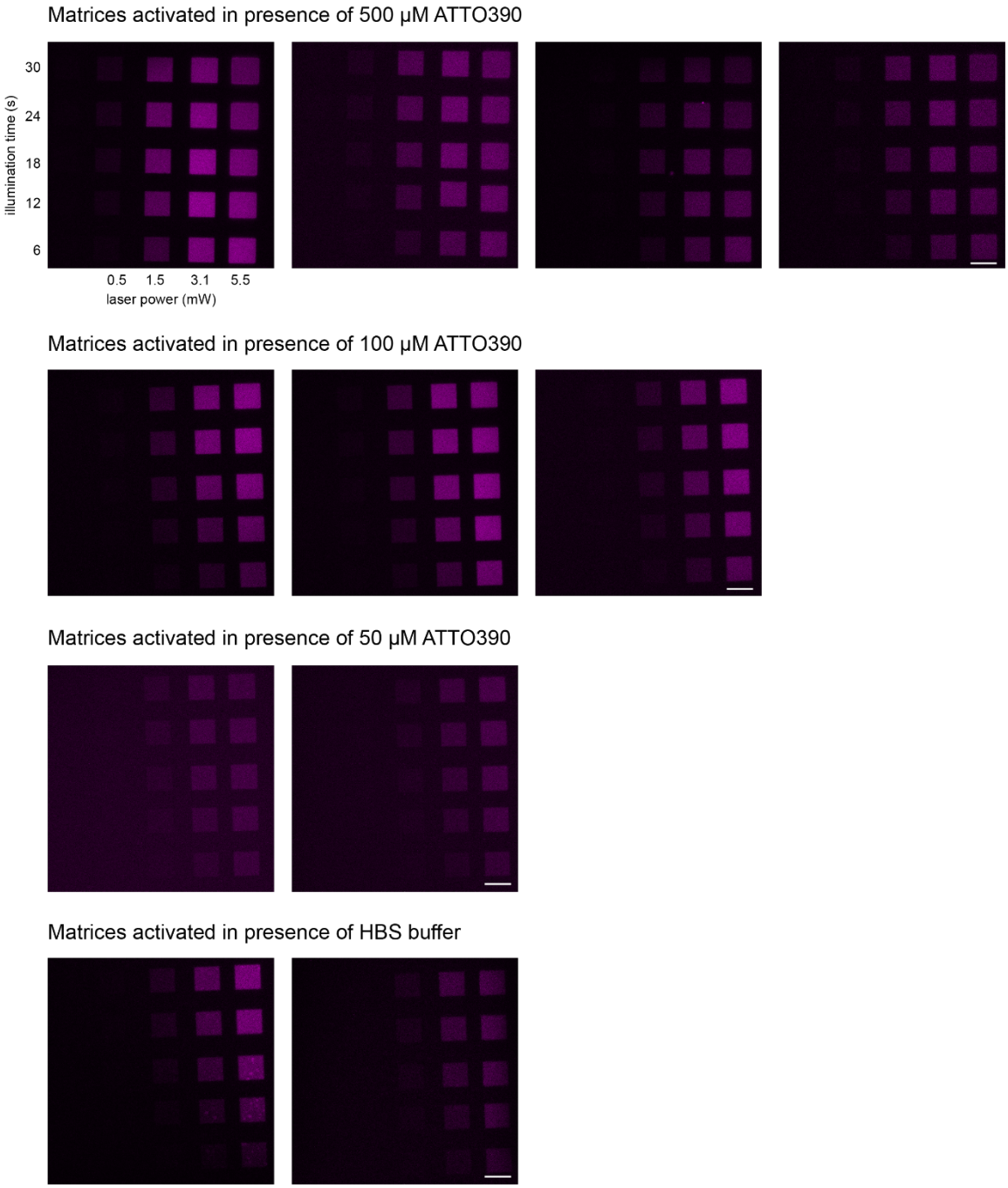

Supplematary Figure 11. ATTO390-sensitized two-photon laser lithography in photo-instructive matrices. TPA-*tris*NTA functionalized hydrogels were photo-activated at 800 nm in the presence of 0, 50, 100 or 500 µM ATTO390 with varying laser power (0.5, 1.5, 3.1 or 5.5 mW) and illumination time (6-30 s). Representative photo-structured gels for all ATTO390 concentrations were shown, with each voxel corresponding to a unique patterning condition. With increased laser power or illumination time, an enhanced tethering of His_6-AF647 was observed, implicating an improved photo-activation of TPA-*tris*NTA. A high ATTO390 concentration in combination with high laser power and illumination time resulted in a halo-effect in the focal plane, induced by plasma-mediated ablation (top row, rightmost top). Overall, the presence of 100 µM ATTO390 induced an intensified photo-scission and consequently enriched POI binding. Images were obtained by confocal laser scanning microscopy and the shown images were not background-corrected. Scale bar: 15 µm.

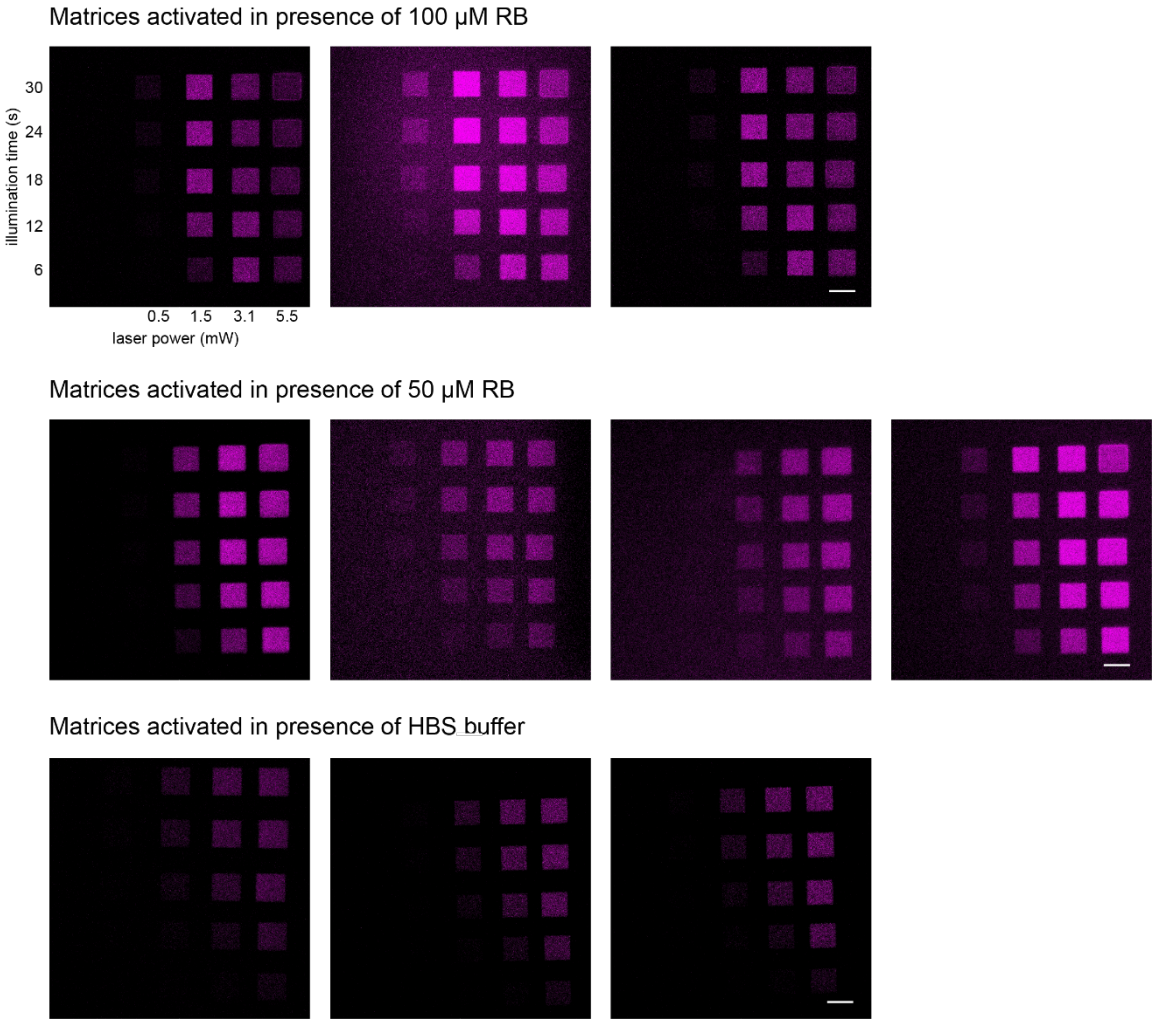

Supplematary Figure 12. Rhodamine B sensitized two-photon laser lithography in photo-instructive matrices. Two-photon excitation of TPA-*tris*NTA functionalized hydrogels was performed at 800 nm in the presence of 0, 50 or 100 µM rhodamine B and increasing both laser power (0.5, 1.5, 3.1 or 5.5 mW) and illumination time (6-30 s). Representative photo-structured gels for all rhodamine B concentrations were shown, with each voxel corresponding to a unique patterning condition. An enhanced binding of His_6-AF647 in response to elevated laser power and illumination time indicates an improved photo-activation of TPA-*tris*NTA. At 100 µM rhodamine B, destructive photo-artifacts induced by plasma-mediated ablation occurred more frequently (top row). A halo-effect in the focal plane was already observed with 50 µM rhodamine B plus increased laser power and extended illumination time (middle row, rightmost top). Collectively, the presence of 50 µM rhodamine B induced an intensified photo-scission and thus enriched POI binding. Confocal laser scanning microscopy was employed to visualize the gels and images were not background corrected. Scale bar: 15 µm.

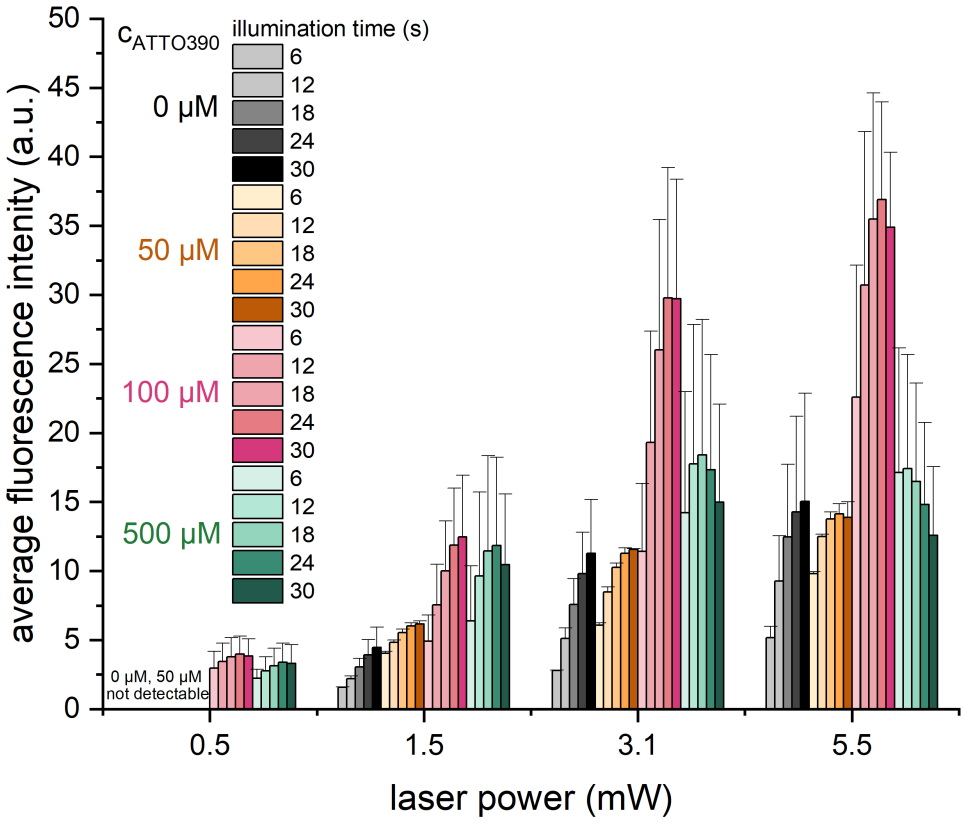

Supplematary Figure 13. Quantification of ATTO390-sensitized two-photon patterned hydrogels via fluorescence intensity analysis. Photo-instructive hydrogels photo-activated at 800 nm in presence of 0, 50, 100 or 500 µM ATTO390 and visualized by tethering of His_6-AF647 were imaged by confocal laser scanning microscopy. Z stacks (35 slices, z step width 1 µm) of the photo-structured ROIs were recorded to cover the entire photo-activated area. After background correction, the total integrated fluorescence intensity within each voxel was determined by calculating the sum over all z slices, which was performed for each ATTO390 concentration and photo-activation condition. Integrated fluorescence densities obtained under equal conditions were averaged and reported in a bar diagram. Optimal two-photon patterning conditions, maximizing total immobilized His_6-tagged POI quantity as well as z resolution while minimizing illumination time, were identified as 3.1 mW with 12 s illumination time and 100 µM ATTO390. All experiments were performed at least in triplicates and error bars indicate the s.d.

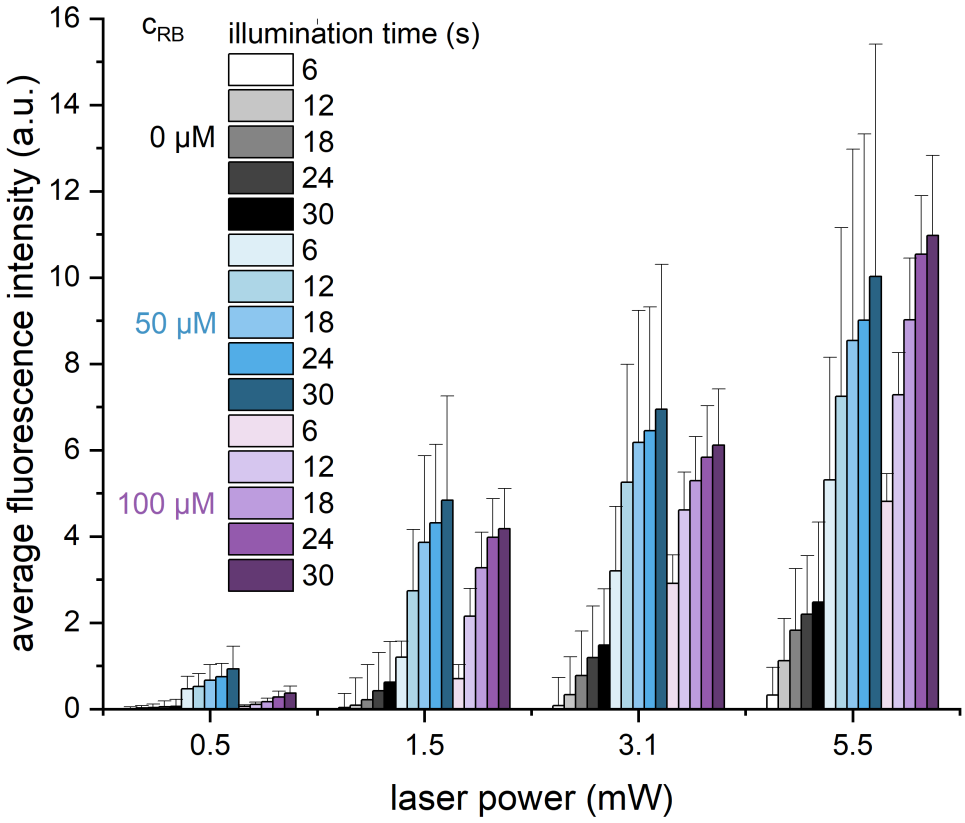

Supplematary Figure 14. Quantification of rhodamine B-sensitized two-photon patterned hydrogels via fluorescence intensity analysis. In presence of 0, 50 or 100 µM rhodamine B, photo-instructive hydrogels were 2P-patterned at 800 nm followed by binding of His_6-AF647 and visualization via confocal laser scanning microscopy. Z stacks (35 slices, z step width 1 µm) of the photo-structured ROIs were recorded to cover the entire photo-activated area. After background correction, the total integrated fluorescence intensity within each voxel was determined by calculating the sum over all z slices, which was performed for each rhodamine B concentration and photo-activation condition. Integrated fluorescence densities obtained under equal conditions were averaged and reported in a bar diagram. Optimal two-photon patterning conditions, maximizing total immobilized His_6-tagged POI quantity as well as z resolution while minimizing illumination time, were identified as 3.1 mW with 12 s illumination time and 50 µM rhodamine B. All experiments were performed at least in triplicates and error bars indicate the s.d.

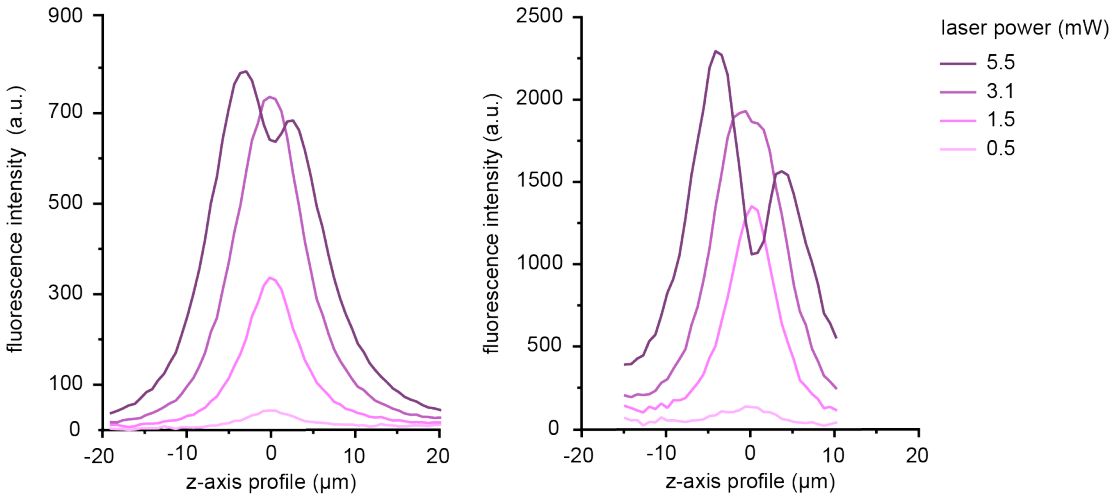

Supplematary Figure 15. Z axis intensity profiles of 2P-patterned hydrogels in presence of photo-sensitizers. Two-photon laser lithography (λ = 800 nm) in presence of 100 µM ATTO390 (left) or 50 µM rhodamine B (right) was exploited in the photo-guided immobilization of His_6-AF647 within TPA-*tris*NTA functionalized hydrogels. Rectangular ROIs were written with increasing laser power (0.5-5.5 mW) for 12 s. After recording a z stack of the ROIs, an orthogonal cross section (x/z plane) of the 2P-activated area was generated followed by performing an intensity line scan profile along the z coordinate. For comparison, the voxel hub is centered at 0 µm. Upon increasing laser power, an enhanced POI tethering was obtained, indicated by the increased fluorescence intensities. At 5.5 mW, a minimum in the intensity profile for both photo-sensitizers was observed as a result of plasma-mediated ablation in the focal plane. Overall, a 15.6-fold improved POI immobilization (reported by the higher total fluorescence intensity) was received by the presence of 50 µM rhodamine B during laser lithography compared to a 3.8-fold enhanced POI tethering with 100 µM ATTO390.

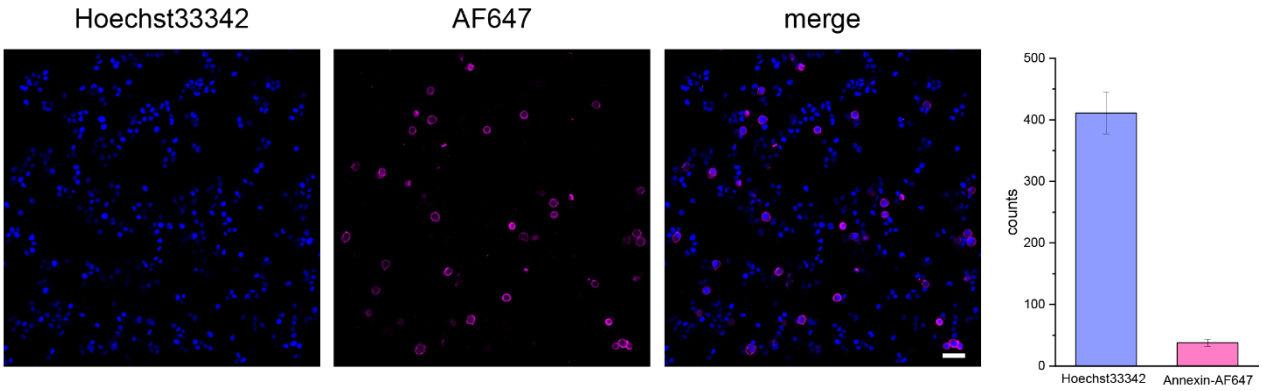

Supplematary Figure 16. Cell viability assessed in cell-laden hydrogels. Living HeLa cells were homogenized with a solution containing TPA-*tris*NTA functionalized polymers and cross-linked to form a cell-laden hydrogel. The encapsulated HeLa cells were treated by annexin V staining to report on apoptotic cells and nuclei were stained with Hoechst33342 to visualize the total amount of cells. Comparison of Hoechst-stained cells *versus* AF647-stained cells revealed that 9% ± 1% of the cells were in an early apoptosis state. The high cell viability of 91 ± 1% confirms that cell embedment in the photo-instructive gel is non-toxic. Imaging was conducted by confocal laser scanning microscopy and analysis was performed with *Fiji*. During imaging the hydrogel was covered with Live Cell Imaging Solution (Invitrogen). Scale bar: 50 µm.

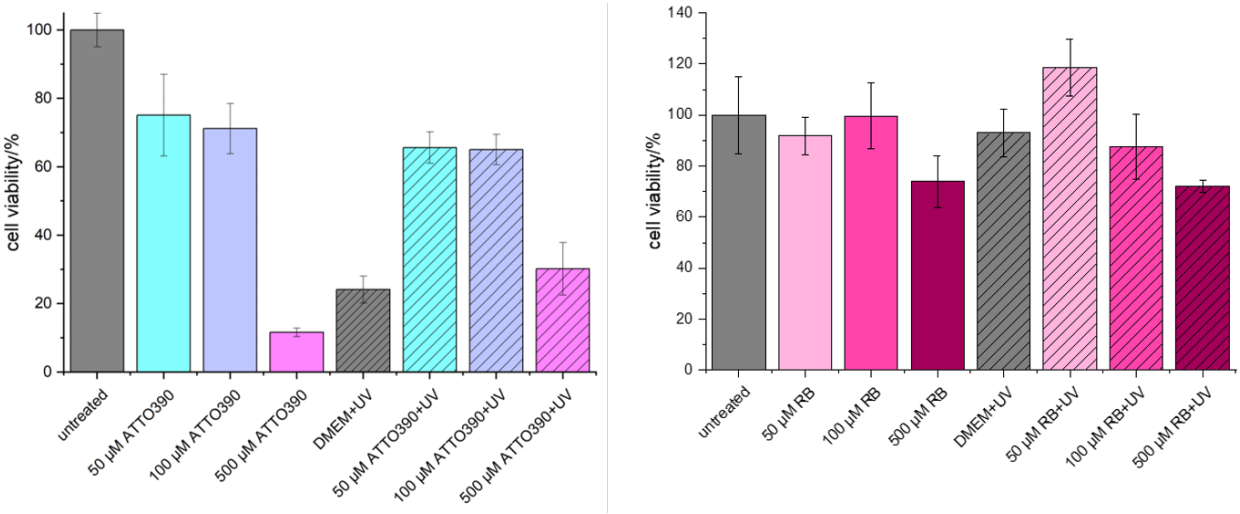

Supplematary Figure 17. Cytotoxicity effect of photo-sensitizers. HeLa cells ($1x10^6$ cells/well) were seeded in 96-well plates and exposed to increasing concentrations of either ATTO390 (0, 50, 100, 500 µM) or rhodamine B (0, 50, 100 µM). Cells were illuminated for 1 min at 365 nm with 185 mW/cm^2 with a custom-made 96-well LED setup and incubated for 2 h. Thereafter, the medium was replaced and cells cultivated for 24 h. Cytotoxicity was assessed via the MTT assay. Untreated cells served as reference. Both compounds showed the absence of dark toxicity up to 100 µM of the photo-sensitizer (ATTO390: > 70% cell viability; rhodamine B: > 70% cell viability). At 500 µM ATTO390, a cytotoxic effect was detected, both in the illuminated and non-illuminated state. In contrast, 500 µM rhodamine B had no cytotoxic effect at all (>70% of viable cells). Collectively, both sensitizers showed cytocompatibility at the applied concentrations (100 µM ATTO390; 50 µM rhodamine B) in the dark as well as under light actuation.

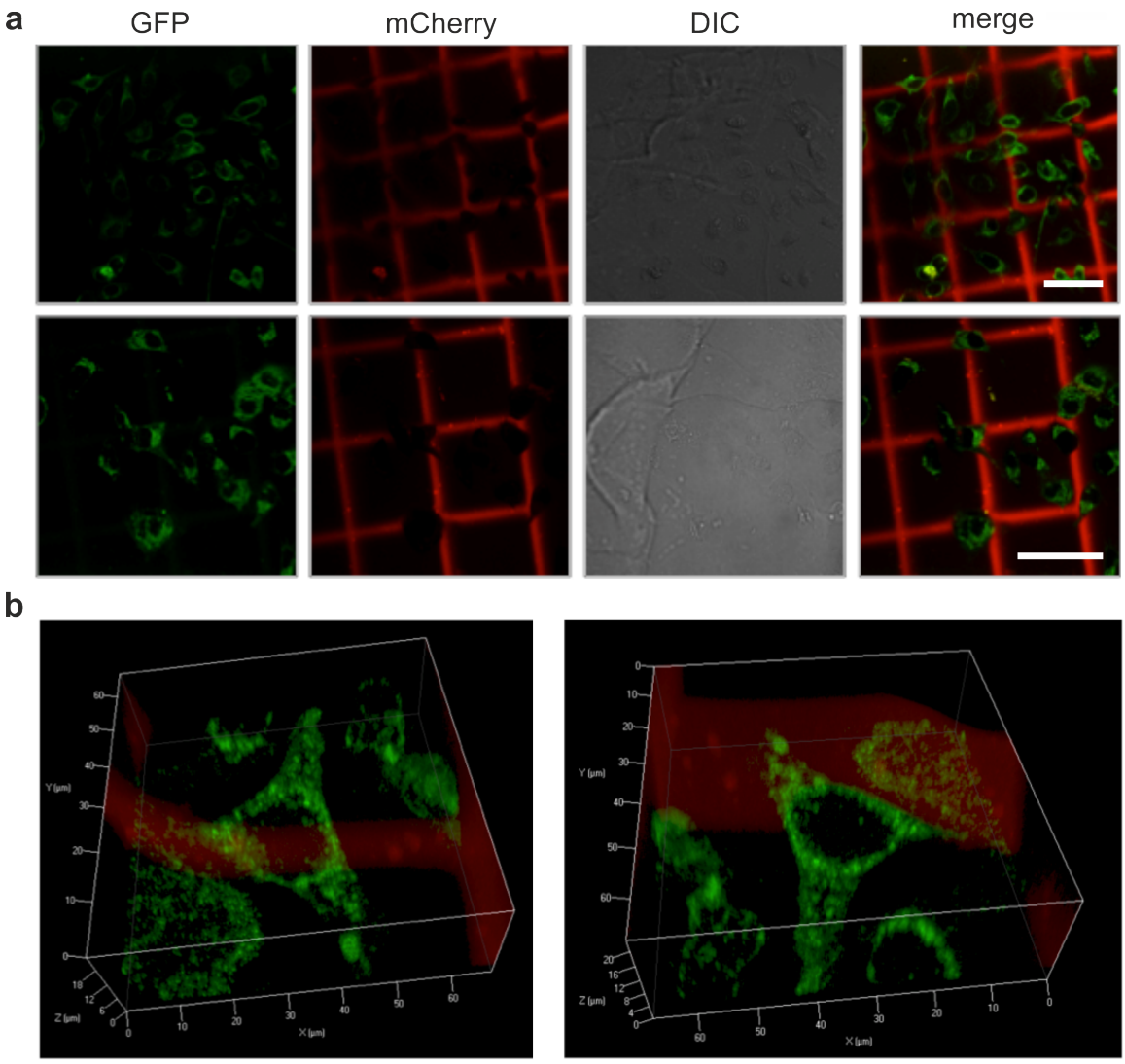

Supplematary Figure 18. One-photon guided protein immobilization in cell-laden, photoinstructive hydrogels. a, Mask patterning of lattice-designed structures using a 405 nm UV/LED system (185 mW/cm^2 for 60 s) was performed in presence of living HeLa cells expressing Y_2R^{mEGFP} and embedded in a photoinstructive hydrogel and followed by POI tethering of His_6-mCherry (300 nM in HBS buffer pH 7.2). Photopatterning and subsequent protein immobilization was visualized by CLSM, demonstrating structuring of large 3D hydrogel areas with His_6-POIs as well as covering multiple living HeLa cells at once. Scale bars: 50 µm. **b,** 3D POI network constructed *via* mask patterning by one-photon activation of TPA-*tris*NTA. Mask patterned structures were visualized by immobilization of His_6-mCherry, and images were reconstructed from a series of z stacks. Photopatterning occurred in three dimensions with uniform organization of His_6-mCherry.

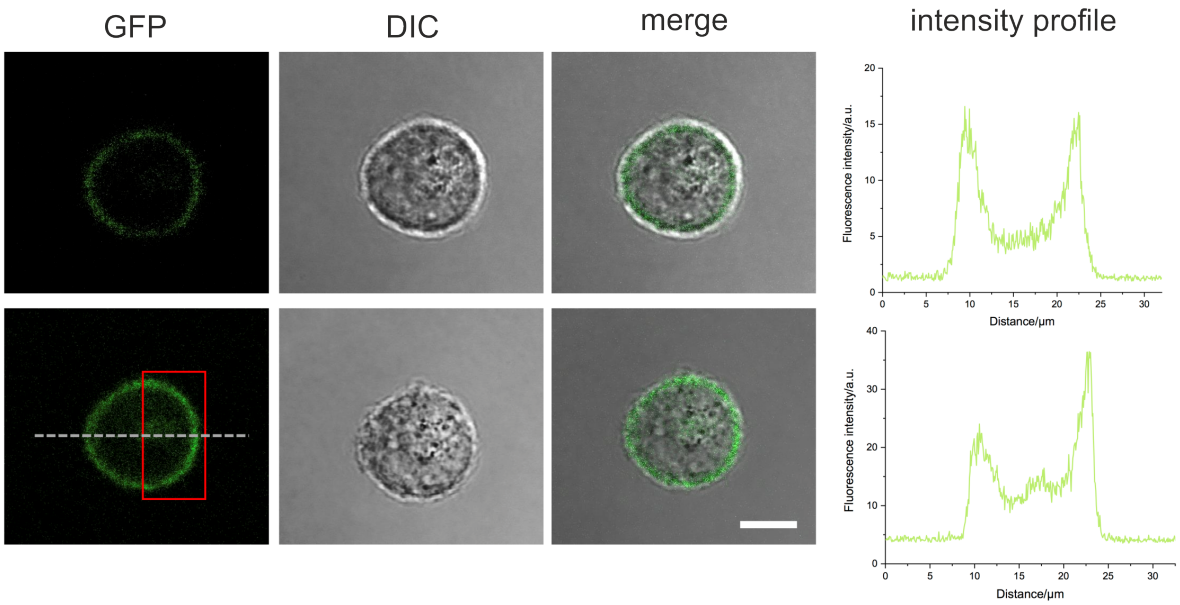

Supplematary Figure 19. Light-induced receptor assembly of HeLa cells expressing His_6-Y_2R^{mEGFP} in photoinstructive hydrogels. One hemisphere of a single cell (red box) embedded in a photoinstructive matrix was illuminated with 405 nm at 4.5 mW/cm^2 laser power and 200 s illumination time). Before illumination, a homogeneous distribution of the receptor was detected (upper row). 30 min after illumination, enrichment of the His_6-tagged receptor at the photoactivated ROI was observed (lower row). Intensity line scan profiles along the cell center were executed (right side). An enhanced receptor assembly at the photoactivated area was observed, expressed by the increased fluorescence intensisty at the light-exposed hemisphere. This indicates receptor enrichment *via tris*NTA/His-tag interaction at the photoactivated area of the cell. a.u. corrssponds to arbitrary units. DIC stands for Differential Interference Contrast. Scale bar: 10 µm.

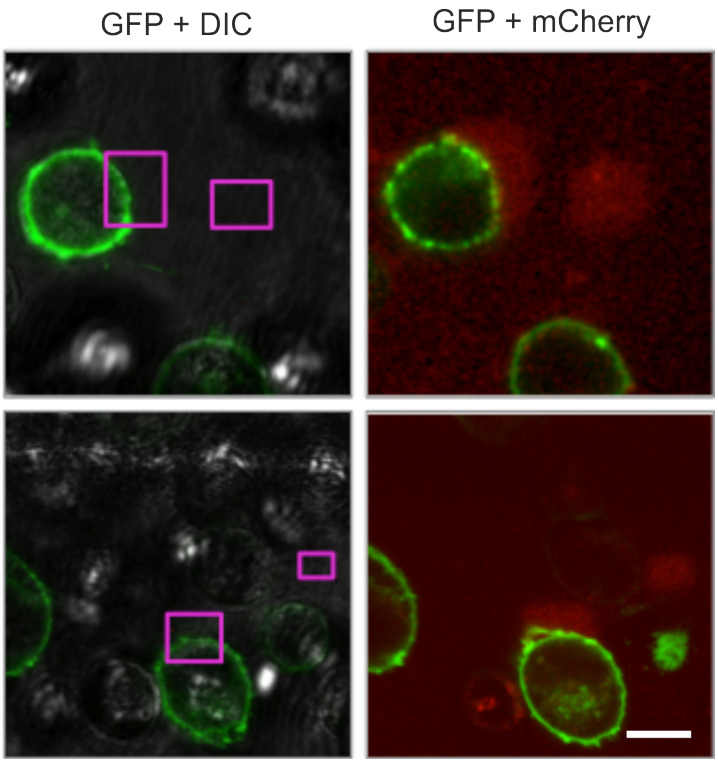

Supplematary Figure 20. Two-photon induced subcellular protein deposition in a cell-laden, photoinstructive TPA-*tris*NTA matrix. Two-photon laser lithography (800 nm, 3.1 mW, 18 s) at defined ROIs (magenta boxes) and subsequent assembly of His_6-mCherry (300 nM in HBS buffer pH 7.2) to living cells embedded in a photoinstructive hydrogel was performed. Images displayed a spatially localized activation of TPA-*tris*NTA at µm-scale and showed a specific immobilization of His_6-POI. In close proximity to live, intact cells, protein deposition confined to gel subvolumes *via* site-specific *tris*NTA/His-tag interaction was realized. Scale bar: 10 µm.

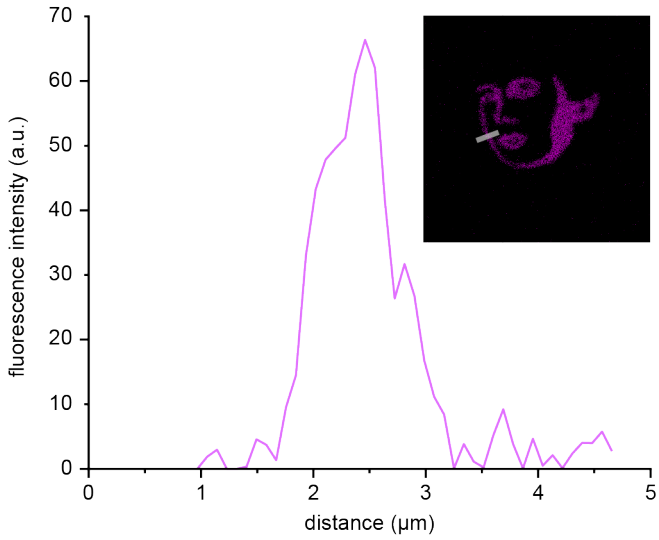

Supplematary Figure 21. Two-photon activation of TPA-*tris*NTA in photo-instructive hydrogels with micrometer precision. A 3D arbitrary POI-pattern (face of Maria Goeppert-Mayer) was generated by two-photon excitation (λ = 800 nm; 3.1 mW, 12 s illumination; 50 µM rhodamine B) and visualized via tethering of 300 nM His_6-AF647. After recording a z stack through the corresponding focal plane, an intensity line scan profile (gray line) in x/y dimension along the cheek of Maria Goeppert-Mayer was performed. Feature sizes with micrometer precision (FWHM ~1 µm) could be written with very good signal-to-background ratio between patterned and non-patterned areas. The result is a combination of the improved two-photon lithography as well as high-affinity, site-selective binding of the photo-liberated *tris*NTA to the His-tagged POI.

3 NMR and mass spectra

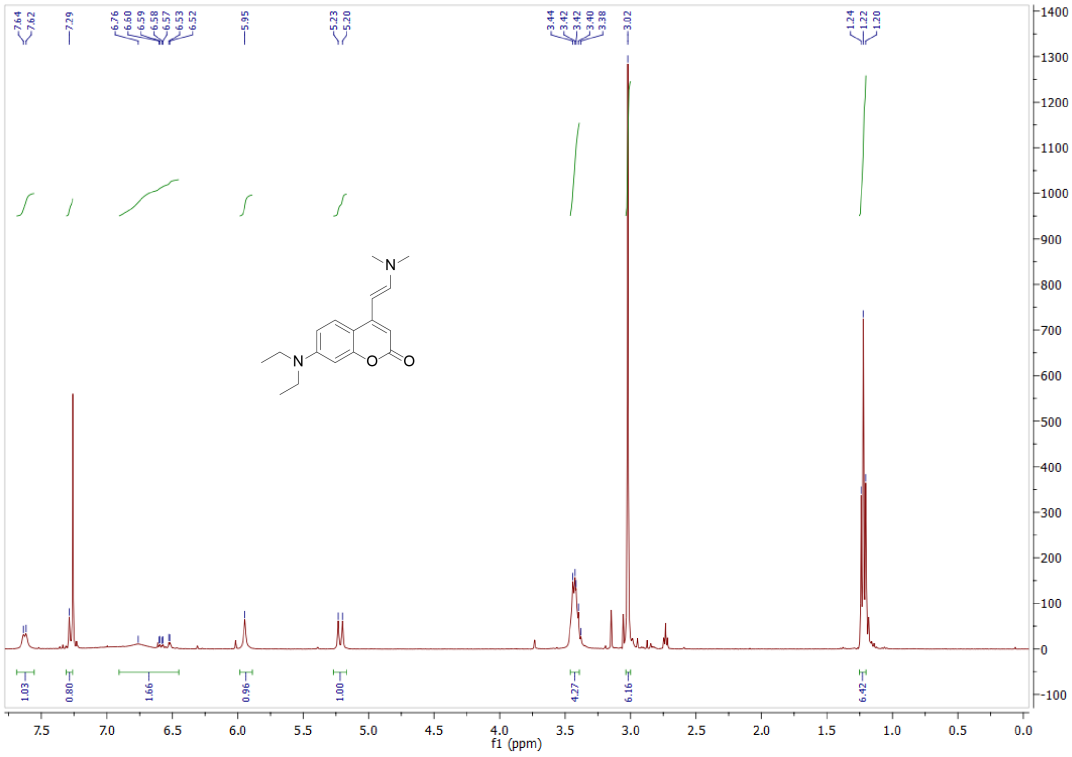

Supplematary Figure 22. ^{1}H-NMR spectrum of compound 2a. ^{1}H-NMR spectrum was recorded at 400 MHz in $CDCl_3$.

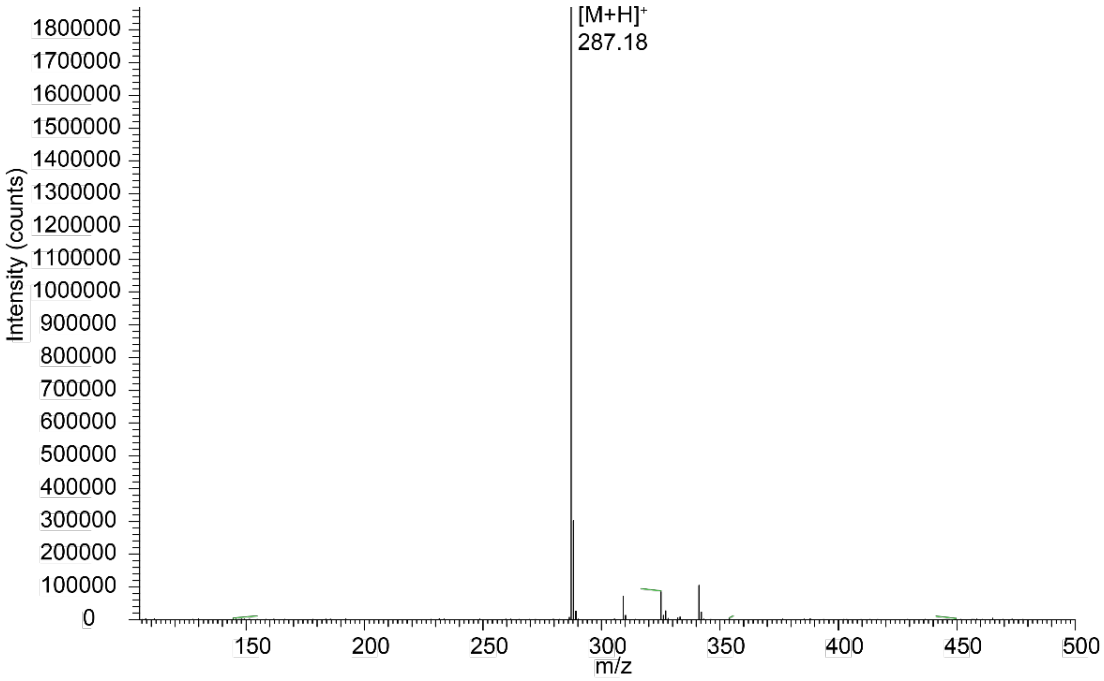

Supplematary Figure 23. ESI-MS spectrum of compound 2a.

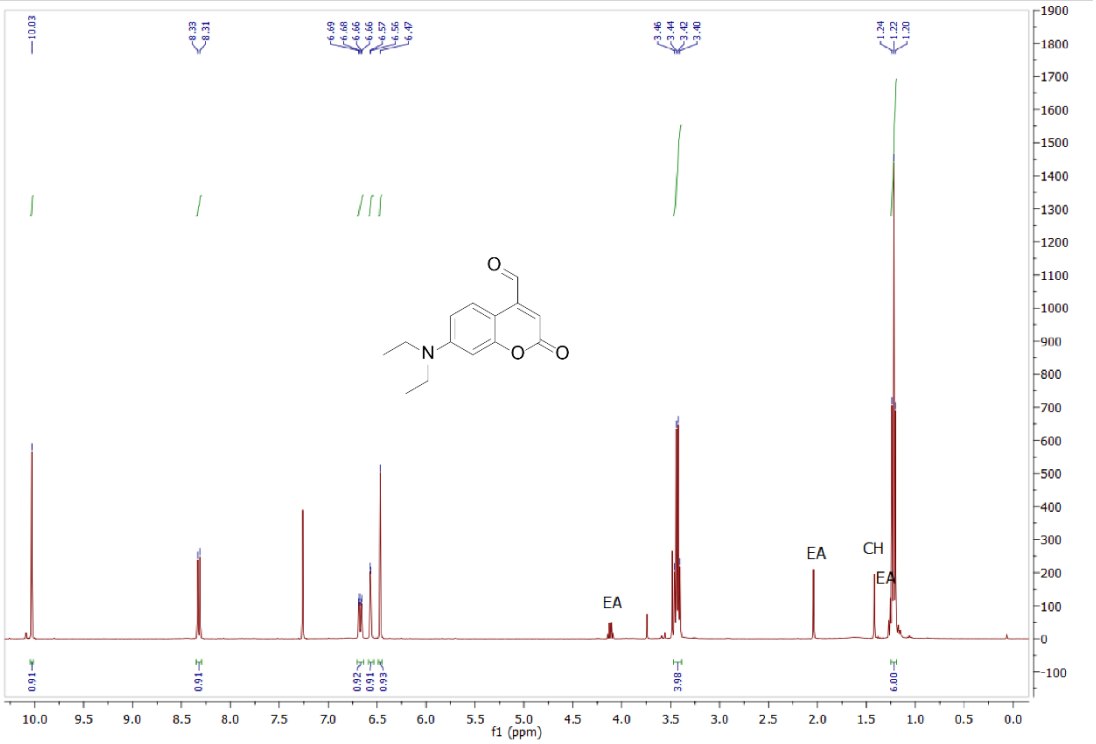

Supplematary Figure 24. ^{1}H-NMR spectrum of compound 2. ^{1}H-NMR spectrum was recorded at 400 MHz in $CDCl_3$.

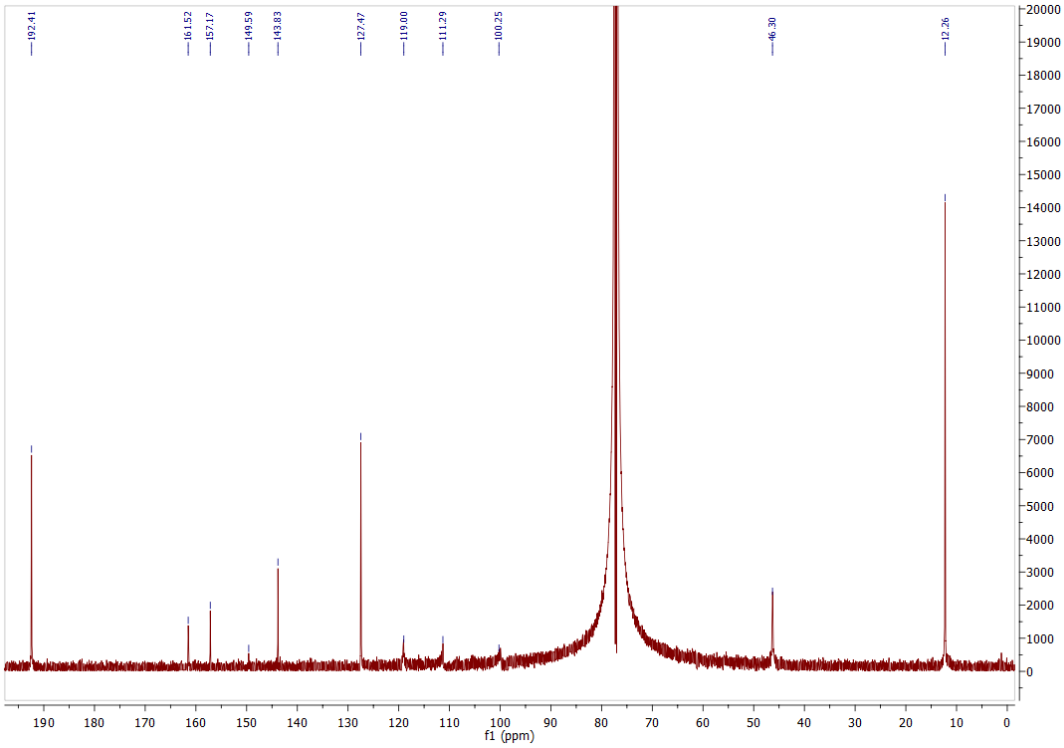

Supplematary Figure 25. ^{13}C-NMR spectrum of compound 2. ^{13}C-NMR spectrum was recorded at 126 MHz in $CDCl_3$.

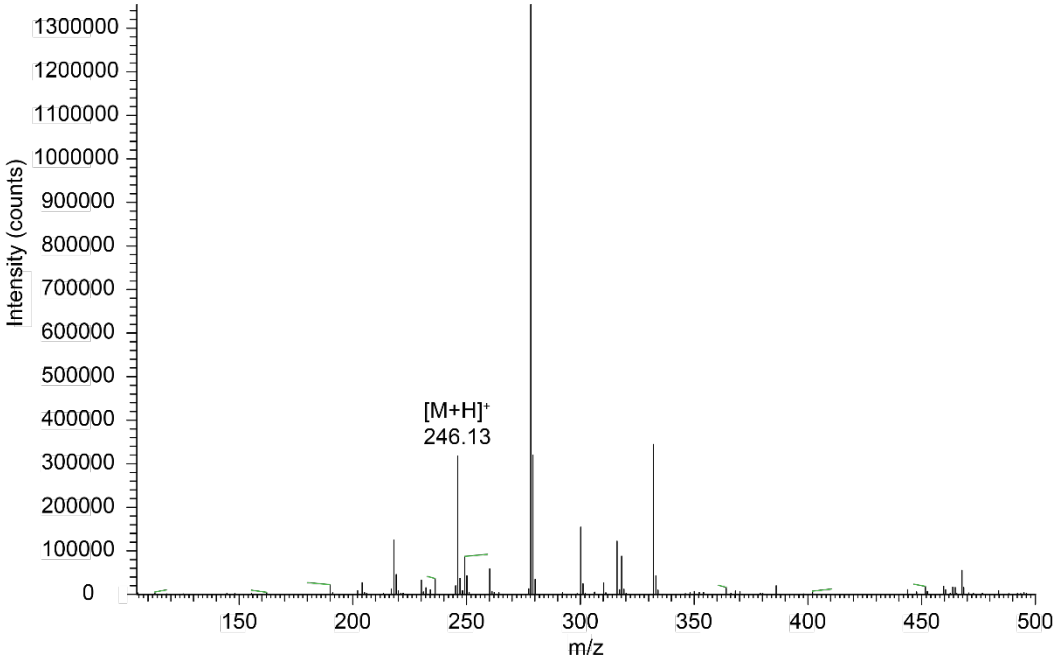

Supplematary Figure 26. ESI-MS spectrum of compound 2.

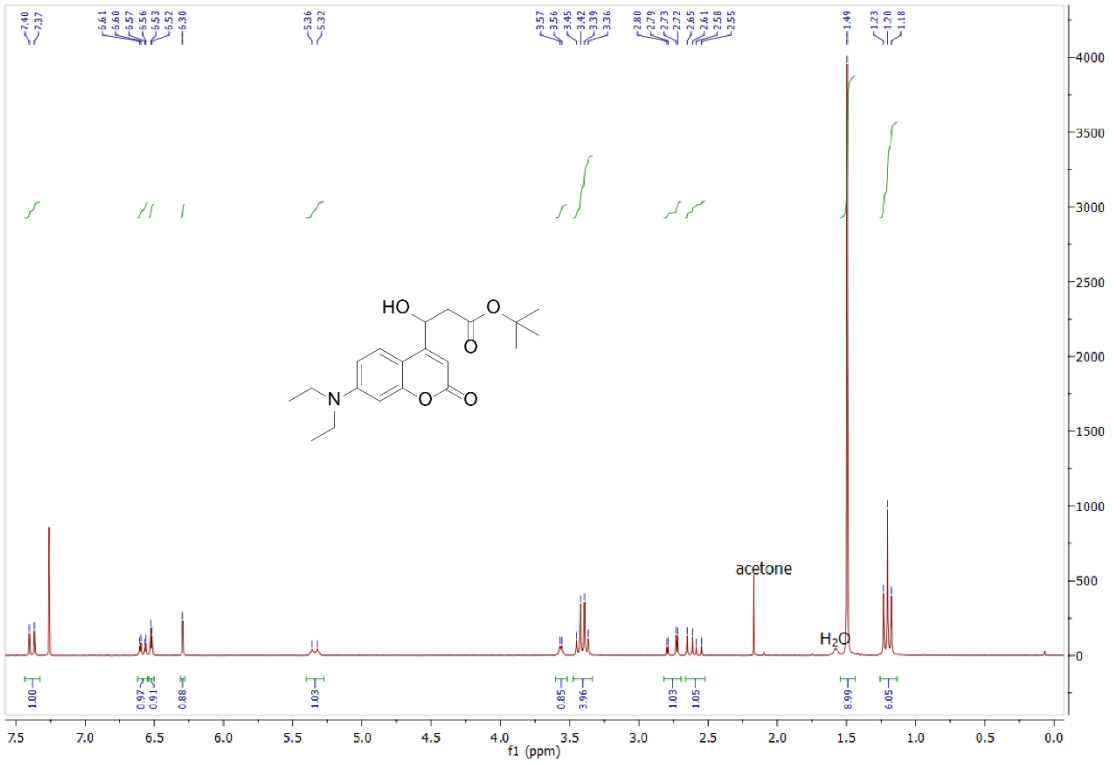

Supplematary Figure 27. ^{1}H-NMR spectrum of compound 3. ^{1}H-NMR spectrum was recorded at 250 MHz in $CDCl_3$.

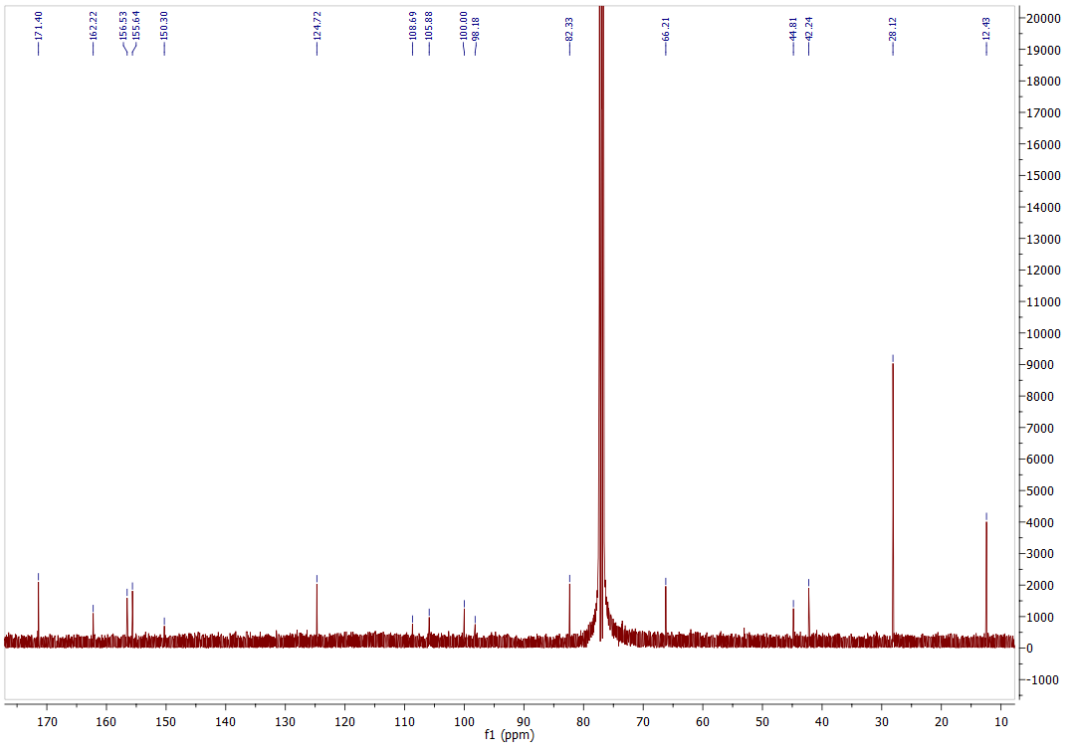

Supplematary Figure 28. ^{13}C-NMR spectrum of compound 3. ^{13}C-NMR spectrum was recorded at 101 MHz in $CDCl_3$.

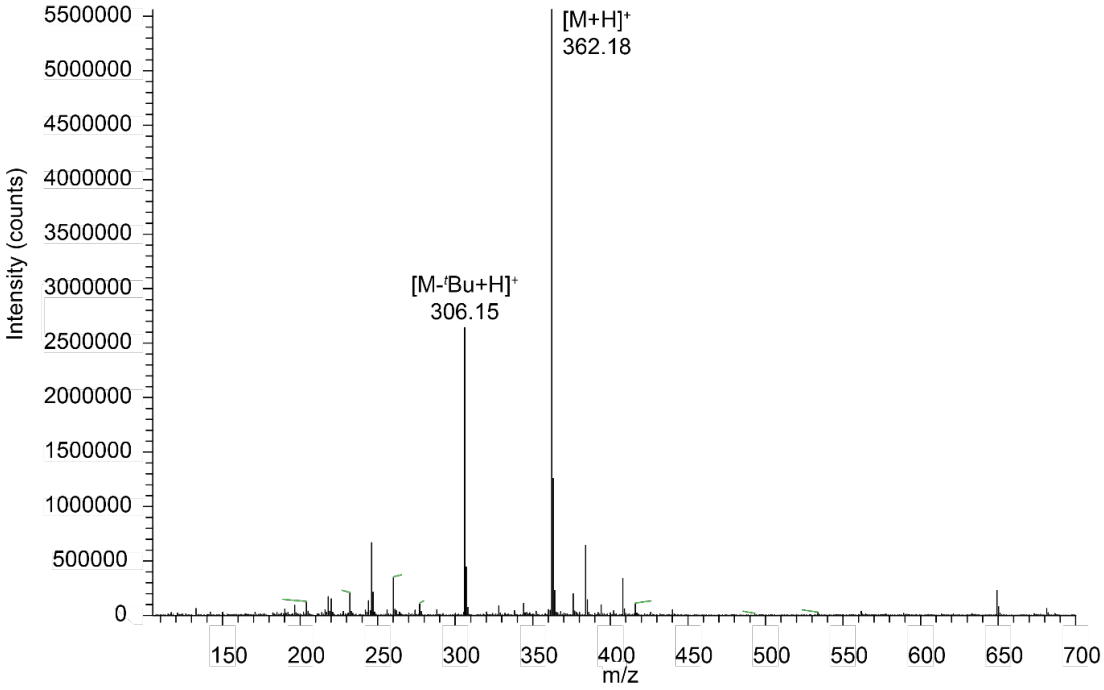

Supplematary Figure 29. ESI-MS spectrum of compound 3.

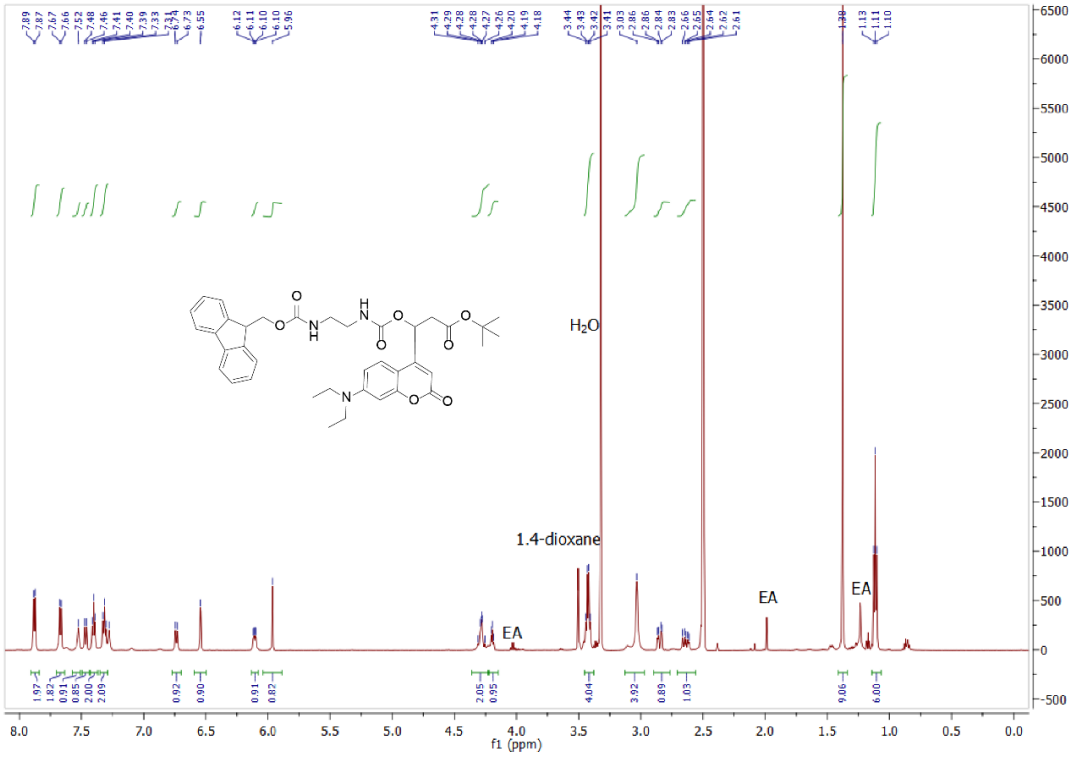

Supplematary Figure 30. ^{1}H-NMR spectrum of compound 3d. ^{1}H-NMR spectrum was recorded at 600 MHz in DMSO-d_6.

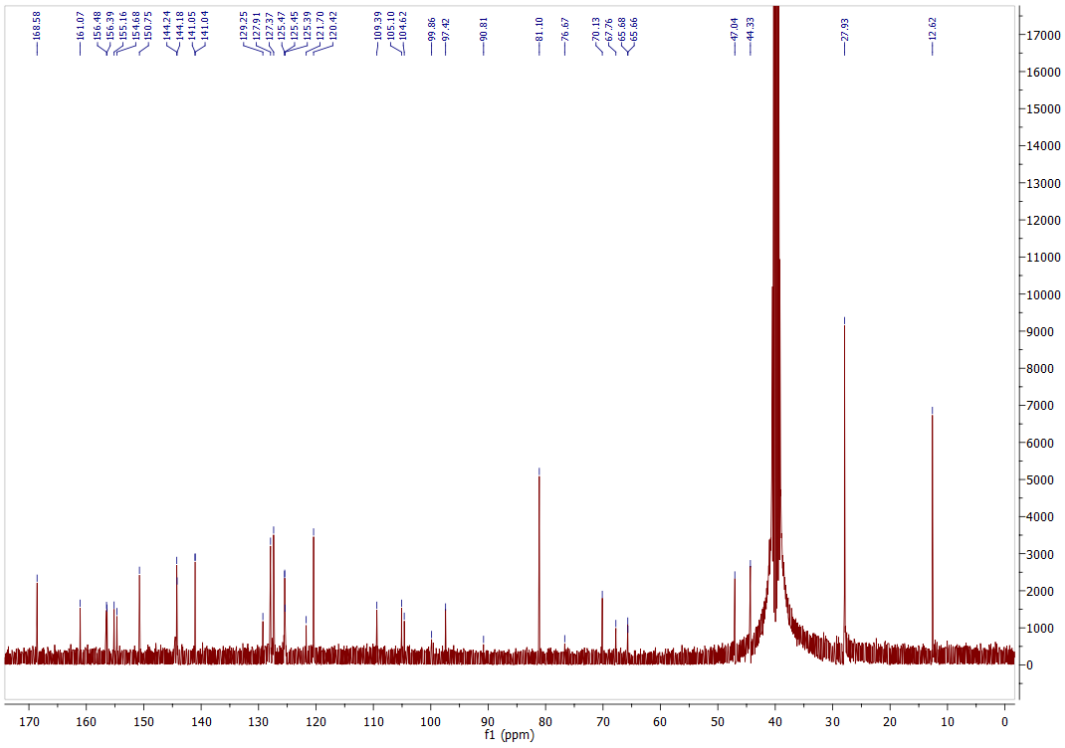

Supplematary Figure 31. ^{13}C-NMR spectrum of compound 3d. ^{13}C-NMR spectrum was recorded at 101 MHz in DMSO-d_6.

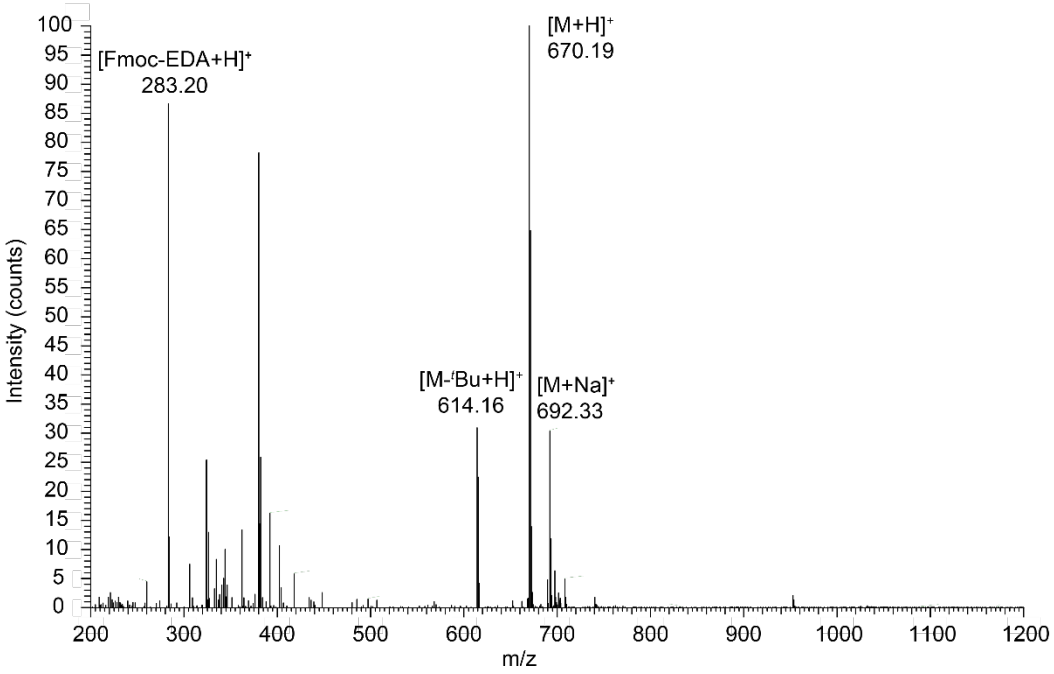

Supplematary Figure 32. ESI-MS spectrum of compound 3d.

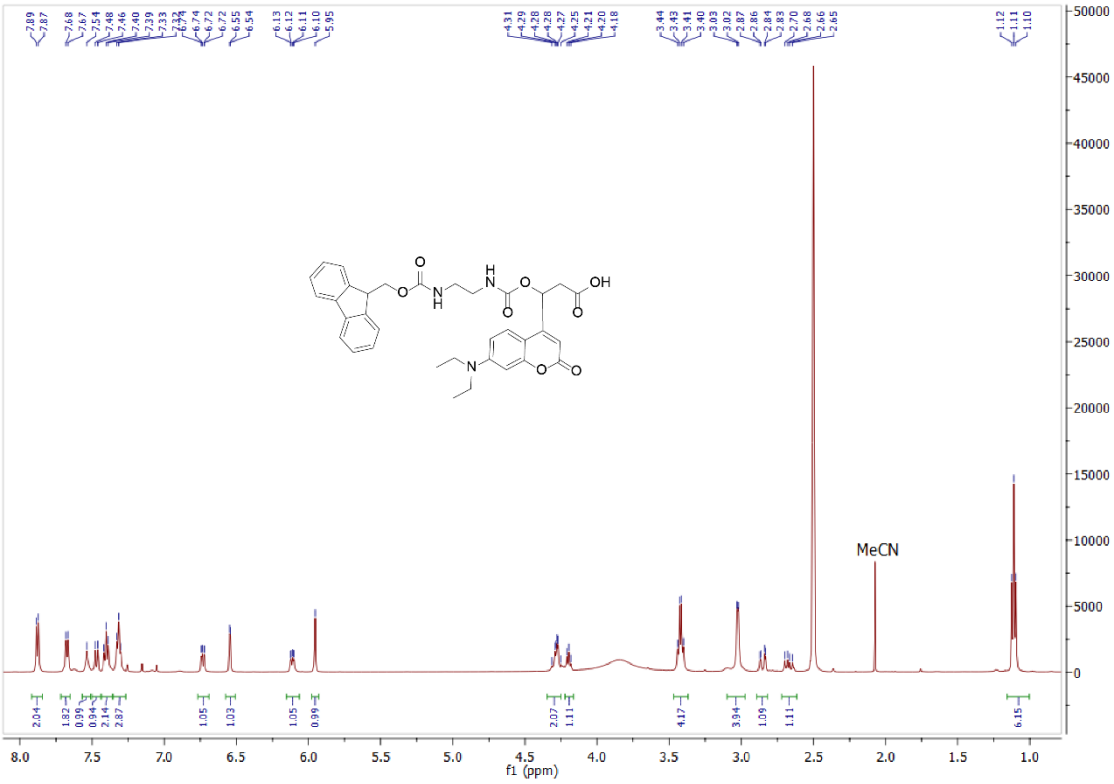

Supplematary Figure 33. ^{1}H-NMR spectrum of compound 4. ^{1}H-NMR spectrum was recorded at 500 MHz in DMSO-d_6.

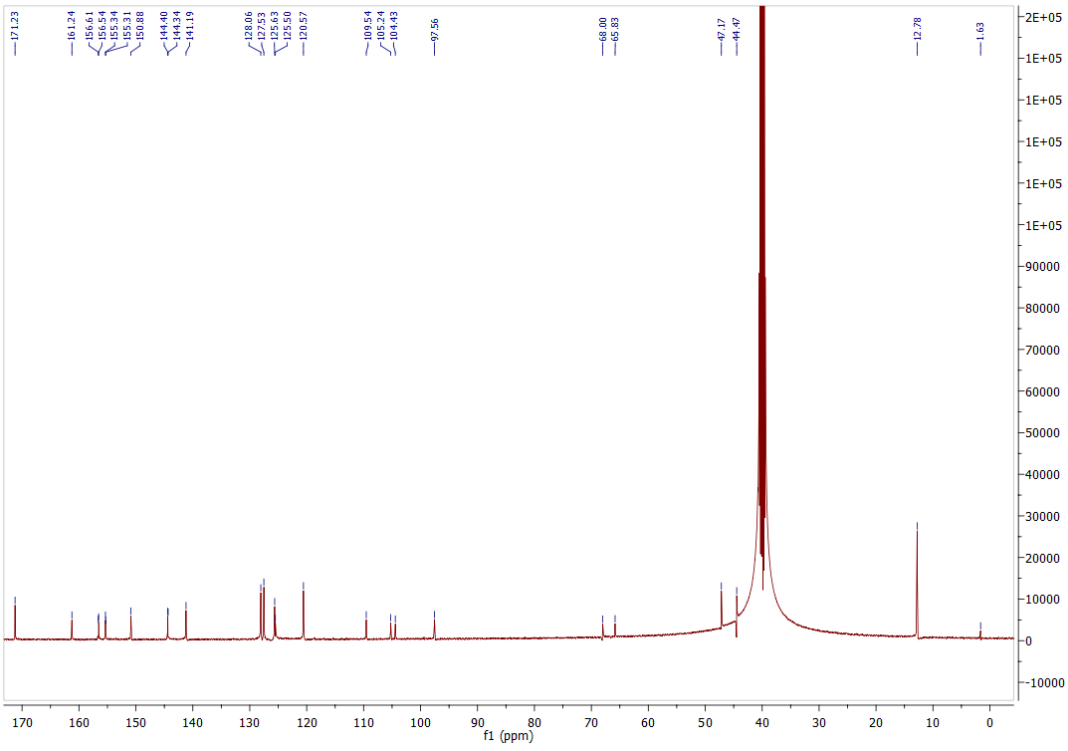

Supplematary Figure 34. ^{13}C-NMR spectrum of compound 4. ^{13}C-NMR spectrum was recorded at 126 MHz in DMSO-d_6.

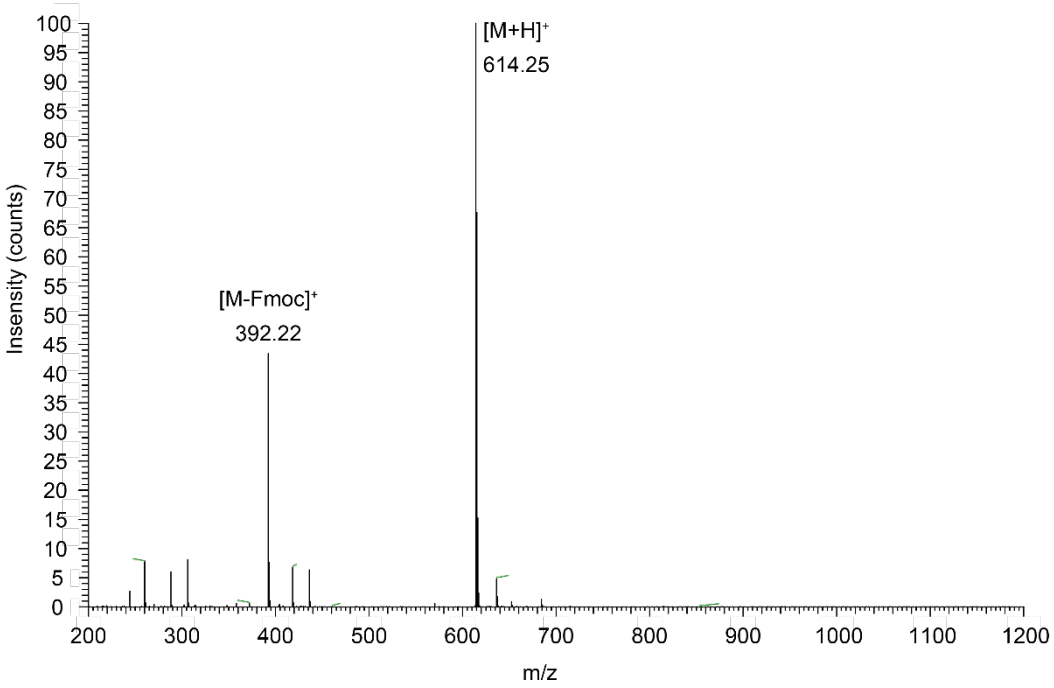

Supplematary Figure 35. ESI-MS spectrum of compound 4.

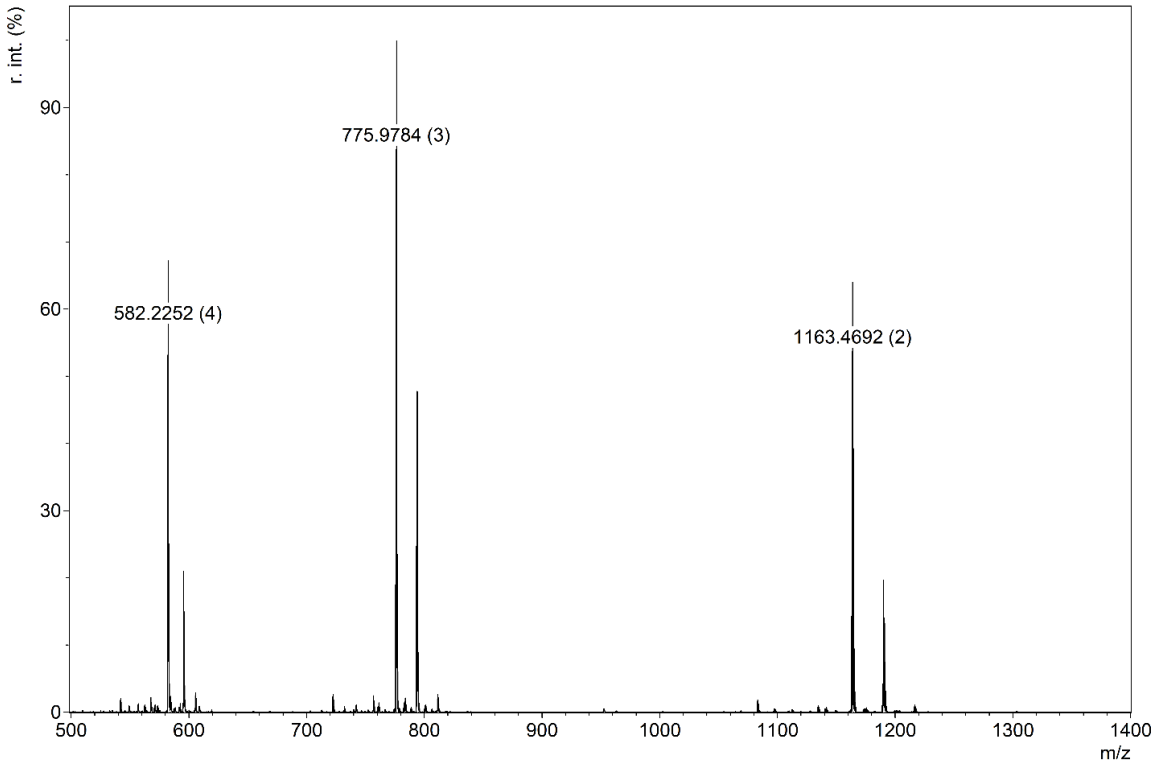

Supplematary Figure 36. HR-ESI-MS spectrum of TPA-*tris*NTA.

4 Supplematary References

1. Lata, S., Reichel, A., Brock, R., Tampé, R. & Piehler, J. High-affinity adaptors for switchable recognition of histidine-tagged proteins. *Journal of the American Chemical Society* **127**, 10205-10215 (2005).

2. Klán, P. et al. Photoremovable Protecting Groups in Chemistry and Biology: Reaction Mechanisms and Efficacy. *Chemical reviews* **113**, 119-191 (2012).

3. Schindelin, J. et al. Fiji: An open-source platform for biological-image analysis. *Nature Methods* **9**, 676-682 (2012).

4. Uphoff, C.C. & Drexler, H.G. Detection of Mycoplasma Contaminations. *Methods in molecular biology (Clifton, N.J.)* **290**, 013-024 (2004).